SCIENTIFIC REPORTS
nature research

OPEN

Novel green synthesis and antioxidant, cytotoxicity, antimicrobial, antidiabetic, anticholinergics, and wound healing properties of cobalt nanoparticles containing *Ziziphora clinopodioides* Lam leaves extract

Huifang Hou[1], Behnam Mahdavi[2]✉, Sogand Paydarfard[2], Mohammad Mahdi Zangeneh[3,4]✉, Akram Zangeneh[3,4], Nastaran Sadeghian[5], Parham Taslimi[6], Vildan Erduran[7] & Fatih Sen[7]✉

The aim of the experiment was a green synthesis of cobalt nanoparticles from the aqueous extract of *Ziziphora clinopodioides* Lam (CoNPs) and assessment of their cytotoxicity, antioxidant, antifungal, antibacterial, and cutaneous wound healing properties. The synthesized CoNPs were characterized using different techniques including UV–Vis., FT-IR spectroscopy, X-ray diffraction (XRD), energy dispersive X-ray spectrometry (EDS), scanning electron microscopy (SEM), and transmission electron microscopy (TEM). According to the XRD analysis, 28.19 nm was measured for the crystal size of NPs. TEM and SEM images exhibited a uniform spherical morphology and average diameters of 29.08 nm for the biosynthesized nanoparticles. Agar diffusion tests were done to determine the antibacterial and antifungal characteristics. Minimum inhibitory concentration (MIC), minimum bactericidal concentration (MBC), and minimum fungicidal concentration (MFC) were specified by macro-broth dilution assay. CoNPs indicated higher antibacterial and antifungal effects than many standard antibiotics ($p \leq 0.01$). Also, CoNPs prevented the growth of all bacteria at 2–4 mg/mL concentrations and removed them at 2–8 mg/mL concentrations ($p \leq 0.01$). In the case of antifungal effects of CoNPs, they inhibited the growth of all fungi at 1–4 mg/mL concentrations and destroyed them at 2–16 mg/mL concentrations ($p \leq 0.01$). The synthesized CoNPs had great cell viability dose-dependently and indicated this method was nontoxic. DPPH free radical scavenging test was done to assess the antioxidant potentials, which revealed similar antioxidant potentials for CoNPs and butylated hydroxytoluene. In vivo experiment, after creating the cutaneous wound, the rats were randomly divided into six groups: untreated control, treatment with Eucerin basal ointment, treatment with 3% tetracycline ointment, treatment with 0.2% $Co(NO_3)_2$ ointment, treatment with 0.2% *Z. clinopodioides* ointment, and treatment with 0.2% CoNPs ointment. These groups were treated for 10 days. For histopathological and biochemical analysis of the healing trend, a 3 × 3 cm section was prepared

[1]School of Basic Medicine, Xinxiang Medical University, Xinxiang 453003, China. [2]Department of Chemistry, Faculty of Science, Hakim Sabzevari University, Sabzevar, Iran. [3]Biotechnology and Medicinal Plants Research Center, Ilam University of Medical Sciences, Ilam, Iran. [4]Department of Clinical Sciences, Faculty of Veterinary Medicine, Razi University, Kermanshah, Iran. [5]Department of Chemistry, Faculty of Sciences, Ataturk University, 25240 Erzurum, Turkey. [6]Department of Biotechnology, Faculty of Science, Bartin University, 74100 Bartin, Turkey. [7]Sen Research Group, Biochemistry Department, Faculty of Arts and Science, Dumlupinar University, Evliya Celebi Campus, 43100 Kutahya, Turkey. ✉email: b.mahdavi@hsu.ac.ir; m.mehdizangeneh@yahoo.com; fatihsen1980@gmail.com

from all dermal thicknesses at day 10. Use of CoNPs ointment in the treatment groups substantially raised ($p \leq 0.01$) the wound contracture, hydroxyl proline, hexosamine, hexuronic acid, fibrocyte, and fibrocytes/fibroblast rate and remarkably decreased ($p \leq 0.01$) the wound area, total cells, neutrophil, and lymphocyte compared to other groups. In conclusion, CoNPs can be used as a medical supplement owing to their non-cytotoxic, antioxidant, antibacterial, antifungal, and cutaneous wound healing effects. Additionally, the novel nanoparticles ($Co(NO_3)_2$ and CoNPs) were good inhibitors of the α-glycosidase, and cholinesterase enzymes.

Nanotechnology and nanoscience are the study and application of extremely small things and can be used across all the other science fields, such as biology, chemistry, physics, materials science, and engineering[1]. Nanotechnology are based on nanoparticles, particles with a 3D structure and a size of 1–100 nm. These materials are available in various sizes and shapes such as crystal, spherical, needle, and rod forms[1]. Different physical, chemical, and biological methods are used to produce nanoparticles. Use of physical methods requires high temperature, pressure, and cost. On the other hand, most chemical methods use chemicals that are toxic and hazardous to the environment and biological systems. Another problem of using this method is the production of toxic products[2]. Hence, there is an increasing need to discover a highly efficient and inexpensive method free of toxins and environmental damage. The biological method is one of the methods that is increasingly being used for the production of nanoparticles[2]. There is a bulky list of sources used in the biological production of metal nanoparticles, including plants and plant extracts[3]. Recently, plants have been increasingly used for the synthesis of nanoparticles. In general, photosynthesis of nanoparticles by plants has many advantages. In photosynthesis of nanoparticles by plant extracts, water is used as a solvent which is free of risk[4]. Biosynthesis of nanoparticles by plant extracts is very easy and does not require specific conditions needed in physical and chemical methods. Plant extracts have a higher reduction potential than microbial culture media, thereby requiring less time for the formation of nanoparticles.[5] The contamination created in biosynthesis of nanoparticles by plant extracts is less than other methods and is approximately zero. Therefore, the biosynthesis of nanoparticles by plant extracts has fewer environmental and is more environmentally friendly[4,5]. However, the production speed, quality, and other characteristics of the nanoparticles produced by plant extracts depend on factors such as nature of plant extract, the concentration of the extract, salt concentration, pH, temperature, and duration of the reaction[6,7]. In previous studies indicated that metallic nanoparticles of plant extract have strong potentials in the treatment of bacterial, fungal, and skin diseases[8–10].

Cutaneous wound healing is a dynamic, complex, and regular response to impairment that requires the interaction of different types of cells, structural proteins, growth factors, and proteinases[11]. The basic principles of cutaneous wound healing are the minimization of tissue damage, adequate blood supply, oxygenation, proper diet, humid environment to create anatomic integrity, and function of the affected site[12]. The cutaneous wound healing process includes accumulation of platelets, coagulation, inflammatory response to damage, changing the underlying materials, angiogenesis, and re-epithelization[12]. Inflammation is a normal phenomenon in the wound healing process and is important for the elimination of the contaminating microorganisms. Prolonged inflammation occurs in the absence of effective decontamination. When microbial cleaning is incomplete, bacteria and endotoxins can prolong the pro-inflammatory cytokines as well as the inflammatory phase[13]. Subcutaneous cells begin to make collagen following injury and regenerate the epithelial cells. Hence, it is therapeutically important to discover methods to accelerate the regeneration of dermis and epidermis against skin injuries[14]. In recent years, the use of chemicals has encouraged the researchers to conduct many studies on the use of traditional and herbal medicines. These studies have revealed that natural drugs are the only treatment modality in some cases, and the compounds available in them have been used in pharmaceutical industries[15]. Since no definitive drug has been introduced for wound healing, it is necessary to perform studies on the effects of herbal drugs and other metal nanoparticles on cutaneous wound healing[15].

Iran has experimental plants that are widely distributed throughout the country, particularly in Kermanshah province, west of Iran (geographical coordinates: 34.3277°N and 47.0778°E)[16–19]. They have been the foundation for inhibition and treatment of experimental a[20–24]. One of the most important herbal medicines that are widely used is *Ziziphora clinopodioides* Lam. It belongs to *Ziziphora* genus and Lamiaceae family with the Persian name of *kakuti-e kuhi* is a perennial plant. In Iran, several hundred species in 49 genera of the Lamiaceae family are scattered[25,26]. *Z. clinopodioides* is used in Iranian traditional medicine for treatment of gastrointestinal disorders, common cold, and inflammations is a member of Labiatae family[25]. Various properties such as antifungal[27], antibacterial[26,28], anti-inflammatory[29], and antioxidant[28,30] have been revealed as the effects of this plant. It has chemical components including flavonoids, α and β pinen, terpenoides, thymol, piperitenone, sis-isopulegone, pulegone, and cineol[26,28,31,32]. According to these compounds, it can be having notable therapeutical effects against various diseases. Due to our ongoing interest on the biosynthesis of metal nanoparticles and heterogeneous catalysts, we wish to report for the first time, green synthesis, detailed morphological, structural, and its catalytic applications of CoNPs synthesized by *Z. clinopodioides* leaves. CoNPs have synthesized with plant extract having the ecofriendly polyphenol which acts as a reducing agent and a capping agent. Also, considering the therapeutical effects of *Z. clinopodioides,* we made an attempt to study the cytotoxicity, antioxidant, antibacterial, antifungal, and cutaneous wound healing effects of CoNPs.

Experimental

Materials. All materials were obtained from Sigma Aldrich chemicals.

Figure 1. Image of *Z. clinopodioides*.

Extraction of *Z. clinopodioides* leaves aqueous extract. *Z. clinopodioides* was collected from Kermanshah city in the west of Iran (Fig. 1).

After complete drying of *Z. clinopodioides* leaves in the dark without humidity for one week, the obtained material was powdered. Of the powder, 200 g was weighed, mixed with 2000 mL (1/10weight/volume ratio) distilled water, heated at 45 °C, and stirred for 2 h. It was then kept at ambient temperature for 24 h. Next, the extract was filtered with Whatman paper #2. The primary extract was fed into a vacuum distillation apparatus (a rotary machine with a vacuum pump), and the solvent was evaporated at 40 °C for 1 h, yielding the condensed extract. To prepare the powder of the extract, the condensed solution was put in the oven for 48 h at 40 °C, and the obtained substance was pulverized[33–35].

Preparation, synthesis and chemical characterization of CoNPs. Biosynthesis of cobalt nanoparticles was carried out according to the previous studies with some modification[36,37]. Firstly, 2.5 g of plant extract was dissolved in 62.5 mL of deionized/distilled water, then 30 mL of $Co(NO_3)_2{\cdot}6H_2O$ with a concentration of 30 mM was added to the solution. The mixture was refluxed for 90 min at 60 °C. Then 5 mL of NaOH 2% was slowly added to the mixture during the reaction time. The color of the solution was changed to brown color. In the next step, the mixture was centrifuged at 6,000 rpm for 15 min. Finally, the residue was dried in an oven for 3 h at 80 °C. The obtained brown powder was kept in a vial for chemical characterization and biological activities.

Different techniques were used to characterize the synthesized CoNPs. The methods include UV–Vis., FT-IR spectroscopy; XRD, SEM, EDS, and TEM techniques. Different parameters of the nanoparticle, such as shape, particle size, fractal dimensions, crystallinity and surface area are obtained by these techniques. The UV–Vis. spectra were obtained by a PhotonixAr 2015 UV–Vis. Spectrophotometer (200–800 nm); The FT-IR spectra were recorded using a Shimadzu FT-IR 8400 in the range of 400–4,000 cm^{-1} (KBr disc); MIRA3TESCAN-XMU was used to report the FE-SEM Images and EDS result. The XRD pattern of CoNPs was recorded in the 2θ range of 20°–80° by a GNR EXPLORER instrument at a voltage of 40 kV, a current of 30 mA, and Cu-Kα radiation (1.5406 Å). The average crystal size of CoNPs was calculated using X-ray diffraction according to the Debye–Scherrer equation

$$D = \frac{k\lambda}{\beta cos\theta}$$

Analysis of cytotoxicity of CoNPs. Human umbilical vein endothelial cells (HUVECs) was used to investigate the efficacy of silver nanoparticles in the culture medium. To this end, the cell line was placed in T25 flasks along with complete culture medium, including DMEM (Dulbecco's Modified Eagle Medium), 10% decamplmaneh fetal bovine serum, and 1% penicillin–streptomycin solution and incubated at 37 °C along with 5% CO_2. After cell density reached 80%, the sample was exposed to 1% of EDTA-trypsin solution. After 3 min incubation at 37 °C along with 5% CO_2 in the cell culture incubator and observing the cells detached from the plate floor, the sample was centrifuged for 5 min at 5,000 rpm and the cell deposition was trypsinized by adding the culture medium. Then, the cell suspensions were counted by Neobar slide after trypan blue staining, and cell toxicity test was done by MTT assay. For this reason, 10,000 HUVEC cells along with 200 µL complete culture medium were added to each 98-plate culture plate. To achieve cells with single layer density, the plate was incubated again at 37 °C along with 5% CO_2. After 80% of cell growth was achieved, the culture medium was

removed and the surface of the cells was irrigated with FBS, and 100 µL double concentration culture medium was added afterward. Then, 100 µL $Co(NO_3)_2$, *Z. clinopodioides*, and CoNPs solution soluble in PBS were added to the well 1 (1000 µg/mL). After mixing $Co(NO_3)_2$, *Z. clinopodioides*, and CoNPs in the culture medium, 100 µL of the first well was removed and added to the second well. Next, 100 µL of the second well was removed and added to well 3. This process was continued up to well 11 so that half of the $Co(NO_3)_2$, *Z. clinopodioides*, and CoNPs were added to each well. Well 12 only contained the cell and single concentration complete culture medium and remained as control. The plate was incubated at 37 °C for 24 h at the presence of 5% CO_2, after which cell toxicity was determined by tetrazolium staining. After that, 10 µL of tetrazolium stain (5 mg/mL) was added to the wells, including the control, and the plate was incubated at 37 °C for 2 h at the presence of 5% CO_2. Then, the stain was removed from the wells and 100 µL of DMSO was added to the wells. The plate was wrapped in an aluminum foil and shaken for 20 min in a shaker. Finally, cell viability was recorded by ELISA reader at a wavelength of 570 nm according to the following formula[38]:

$$\text{Percentage of cell viability (\%)} = \left(\text{Sample Absorbance/Control absorbance}\right) \times 100.$$

Measurement of antioxidant properties of CoNPs by DPPH. To determine the trapping potential of DPPH, different concentrations of the $Co(NO_3)_2$, *Z. clinopodioides*, and CoNPs were mixed with 2 mL 0.004% DPPH solution. The control solution contained 2 mL DPPH and 2 mL ethanol. The solutions were kept in darkness at room temperature for 30 min. Then, the absorption rate of the samples was measured at 517 nm by the following formula compared to the control sample[39]:

$$\text{DPPH free radical scavenging (\%)} = (\text{Control} - \text{Test/Control}) \times 100.$$

Preparation of fungal and bacterial species. *Salmonella typhimurium* (ATCC No. 14028) and *Streptococcus pneumonia* (ATCC No. 49619) were procured as lyophilized from Iranian Research Organization for Science and Technology. Also, four fungal species, namely *Candida albicans* (PFCC No. 89-1000), *Candida glabrata* (PFCC No. 164-665), *Candida krusei* (PFCC No. 52951), *Candida guilliermondii* (PFCC No. 88-1947), and four bacterial species, namely *Pseudomonas aeruginosa* (ATCC No. 27853), *Escherichia coli* O157:H7 (ATCC No. 25922), *Bacillus subtilis* (ATCC No. 6633), and *Staphylococcus aureus* (ATCC No. 25923) were procured as lyophilized from Pasteur Institute of Iran.

Analysis of sensitivity of fungal and bacterial strains to CoNPs. Agar disk-diffusion and well-diffusion methods were used to analyze the antifungal and antibacterial activities. To this end, the prepared microbial suspension with 0.5 McFarland turbidity standard was cultured onto Mueller Hinton Agar and Sabouraud Dextrose Agar in completely sterile conditions. In the well diffusion method, 6-mm wells were created by a Pasteur pipette on the culture medium with constant distances. In the disk diffusion method, 6-mm blank disks were used on agar culture medium. Then, 60 µL of different dilutions of $Co(NO_3)_2$, *Z. clinopodioides*, and CoNPs were added to the wells and disks. In this study, distilled water was negative control and antifungal [Fluconazole (60 mg/mL), Itraconazole (60), Miconazole (60), Amphotericin B (60), Nystatin (60)] and antibacterial [Difloxacin (30 mg/mL), Chloramphenicol (30), Streptomycin (10), Gentamicin (10), Oxytetracycline (30), Ampicillin (10), and Amikacin (25)] antibiotics were positive controls. The zone of growth inhibition was recorded after 24 h of incubation at 37 °C[40].

Macro broth dilution method was used to determine Minimum Inhibitory Concentration (MIC). Different dilutions of $Co(NO_3)_2$, *Z. clinopodioides*, and CoNPs were added to macro broth tubes, following which 60 µL fungal and bacterial suspensions were added and incubated for 24 h at 37 °C. Then, the concentration with minimum dilution and no turbidity was considered MIC[40].

To determine minimum bacterial concentration (MBC) and minimum fungicidal concentration (MFC), 60 µL MIC and three preceding chambers were cultured on Muller Hinton Agar and Sabouraud Dextrose Agar, respectively. After 24 h incubation at 37 °C, the minimum concentration with no fungal and bacterial growth was considered MBC and MFC, respectively. All tests were done in triplet[40].

In vivo design. All animal procedures were approved by standards of Kermanshah Payame Noor University (No. 01/Z/G 1395/12/01) on Humane Care and Use of Laboratory Animals, in accordance with the Research Ethics Committee of the Ministry of Health and Medical Education in Iran (adopted on April 17, 2006), based on the Helsinki Protocol (Helsinki, Finland, 1975). A total of 60 male rats of the same race with the weight of 220 ± 5 g were used in this study. The rats were kept in individual cages at 22 ± 2 °C, in 12:12 h dark–light cycle, and with free access to water and food. The rats were anesthetized by intramuscular administration of 40 mg/kg ketamine. After induction of anesthesia, the hair between the two scapulae was shaven, and 3 × 3 cm of the area was disinfected with 70% ethanol. A wound (2 × 2 cm) was made by a scalpel, which involved the removal of all cutaneous layers. The depth of the wound included dermis and hypodermis (Fig. 2).

After creating the cutaneous wound, the rats were randomly divided into six groups: untreated control, treatment with Eucerin basal ointment, treatment with 3% tetracycline ointment, treatment with 0.2% $Co(NO_3)_2$ ointment, treatment with 0.2% *Z. clinopodioides* ointment, and treatment with 0.2% CoNPs ointment. The ointment was applied to the wound bed for 10 consequent days.

On day 10 after complete anesthesia by inhalation of chloroform in a desiccator, a sample was taken from the wound in each group. Histological sections were equally divided into half, half of which was sent to the laboratory in 10% formalin. After staining the samples by hematoxylin–eosin staining technique, they were analyzed

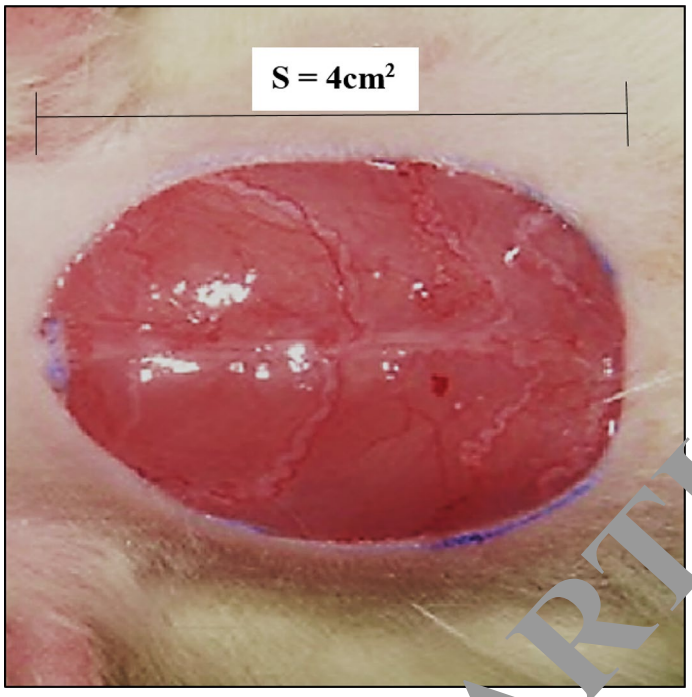

Figure 2. Excision model in rat (S show wound area).

by an optic microscope. In the histopathological study, the number of total cells, blood vessel, fibrocyte, fibroblast, neutrophil, lymphocyte, and macrophage and ratio of fibrocyte to fibroblast were measured. Biochemical studies by determining of hydroxyl proline, hexosamine, and hexuronic acid concentrations were performed on another half of the samples[34].

Enzyme studies. As previously revealed, the inhibition effect of new nanoparticles (CoNPs) on pain and BChE activities was quantified according to Ellman's spectrophotometric method[34]. The α-glycosidase inhibition effect of the new nanoparticles (CoNPs) was adjusted similar to the work of TAO et al.[34]. As mentioned earlier, the absorption values were determined at 405 nm[34].

Statistical analysis. The obtained results were fed into SPSS-22 software and analyzed by one-way ANOVA, followed by Duncan post-hoc test ($P \leq 0.01$).

Results and discussion

Cobalt nanoparticles are used as a therapeutic tool for the treatment of various disease such as microbial infections[41–43]. Therefore, the properties of nanoparticles and their effect on microbes are of great significance in medical applications[41]. Most bacteria have become resistant to antibiotics. Hence, it will be urgent to replace antibiotics with new materials that have antibacterial properties[42,43]. Since low-concentrated cobalt nanoparticles are non-toxic in the body, they are a good substitute for antibiotics[41,43]. These materials in lower concentrations prevent bacterial ad fungal growth and have fewer side effects than antibiotics. There are numerous reports about the use of biological synthesis of cobalt nanoparticles and their antimicrobial activity[41–43]. The present study evaluated the efficacy of CoNPs in the destroying of bacterial and fungal pathogens and healing of cutaneous wound without any cytotoxicity.

Chemical characterization of CoNPs. *UV–visible spectroscopy analysis.* The UV–Vis. spectra of biosynthesized CoNPs using aqueous extract of *Ziziphora* is shown in Fig. 3. The surface plasmon resonance of CoNPs was confirmed by UV–Vis. with observed peaks at 222, 295, and 449 nm which are reported previously[36].

FT-IR analysis. FT-IR spectroscopy is a common technique to identify functional groups of diverse organic compounds based on the peak value in the region of 400–4,000 cm^{-1}. This spectroscopic method is also a sufficient way to recognize the bioactive components in the natural products field. According to the results, a similarity has been observed for FT-IR spectrums of the *Z. clinopodioides* extract and CoNPs (Fig. 4), that could be approved the biosynthesis of the cobalt nanoparticles. The presences of different IR bands related to existences of various functional groups in *Ziziphora* extract. For instance, peaks in 3,377 and 2,933 cm^{-1} related to O–H and aliphatic C–H stretching; the peaks at a range of 1,417 to 1,733 cm^{-1} correspond to C=C and C=O stretching, and peaks at 1,256 and 1,068 cm^{-1} could be ascribed to –C–O and –C–O–C stretching. These peaks could be considered for the presence of various compounds such as phenolic, flavonoid, and carboxylic compounds which have been reported previously[31,44].

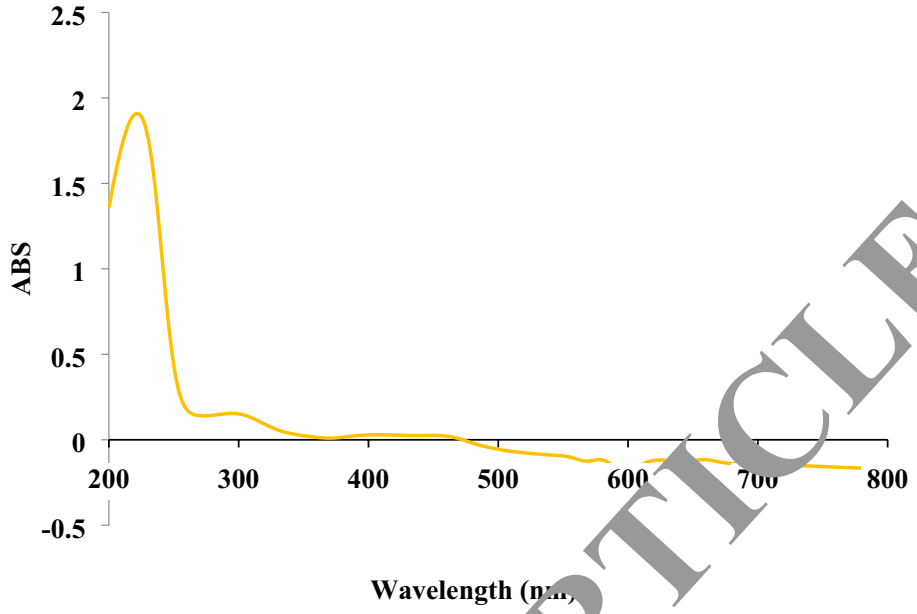

Figure 3. UV–Vis spectra of biosynthesized CoNPs using *Ziziphora* extract.

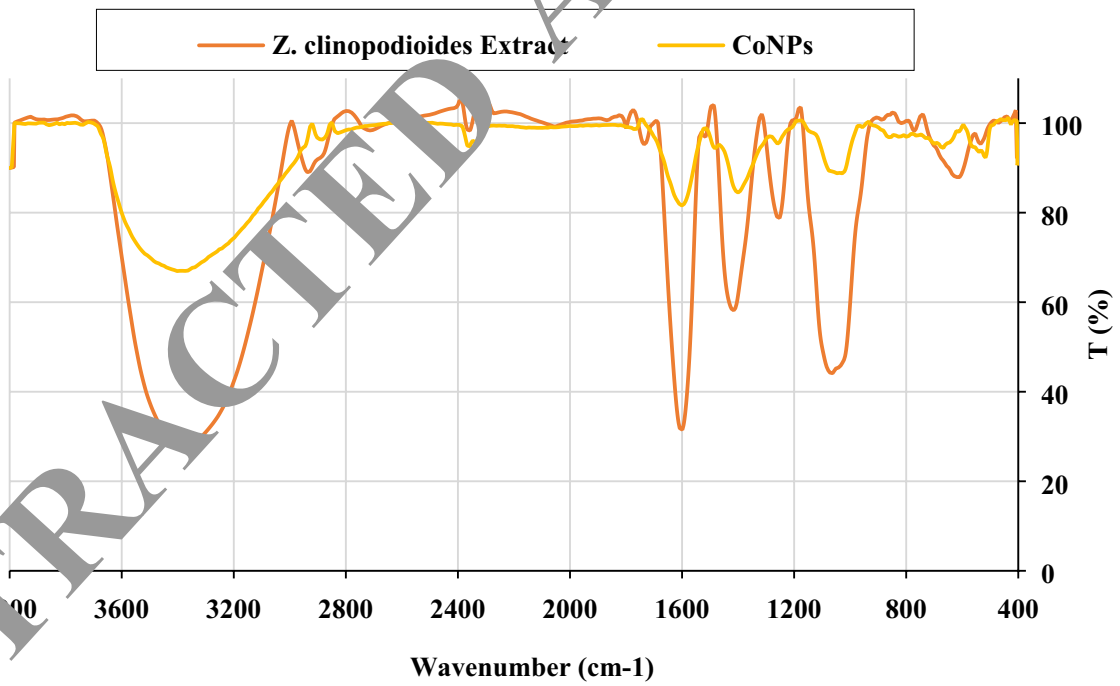

Figure 4. FT-IR spectra of *Ziziphora* extract, and CoNPs.

XRD analysis. The crystallinity of CoNPs was evaluated from the XRD patterns. The diffractogram is shown in Fig. 5. exposes despite the small size of cobalt nanoparticles, they are well crystallized. The attained data were compared with the standard database ICDD PDF card no. 00-015-0806. The peaks at 44.32, 51.38, and 76.15 corresponding to CoNPs (111), (200), and (220) diffraction planes, indicate the formation of CoNPs. The size of the crystals is calculated using Scherrer's formula. It is calculated that the cobalt nanoparticles have an average crystal size of 28.19 nm.

SEM analysis. Field emission scanning electron microscope (FE-SEM) was used to recognize surface morphology and size of CoNPs indicated the formation of homogeneous cobalt NPs with an average diameter size of 29.07 nm. Figure 6a–d show the SEM images of CoNPs in different scales. As it is seen, the nanoparticles are

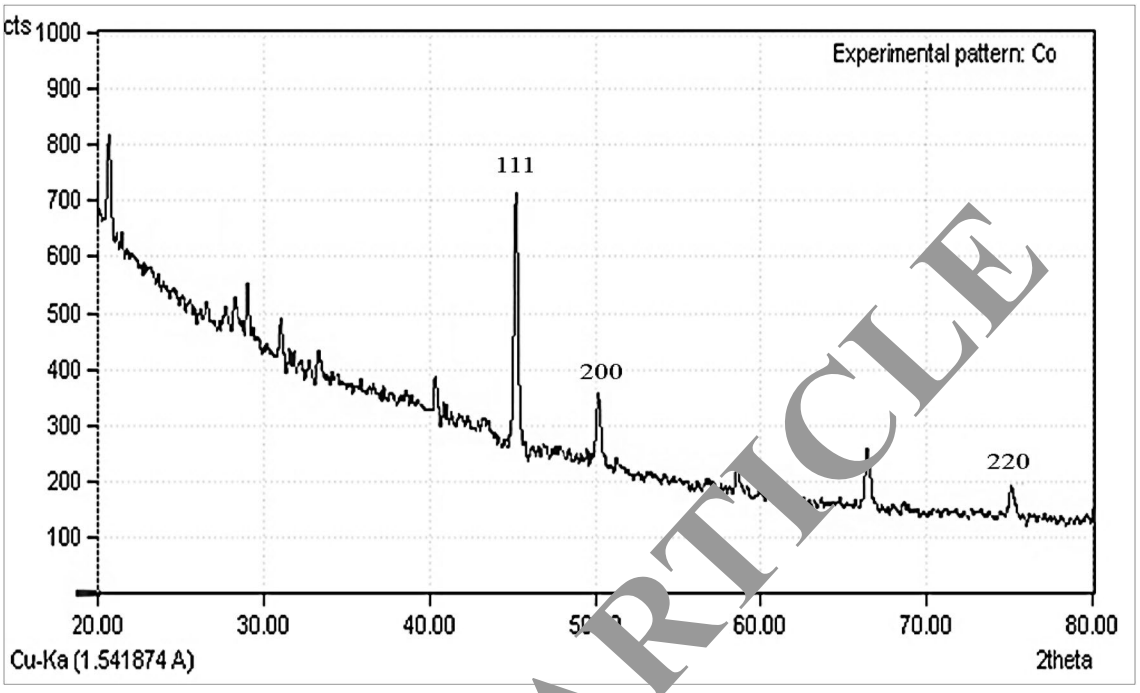

Figure 5. XRD pattern of CoNPs.

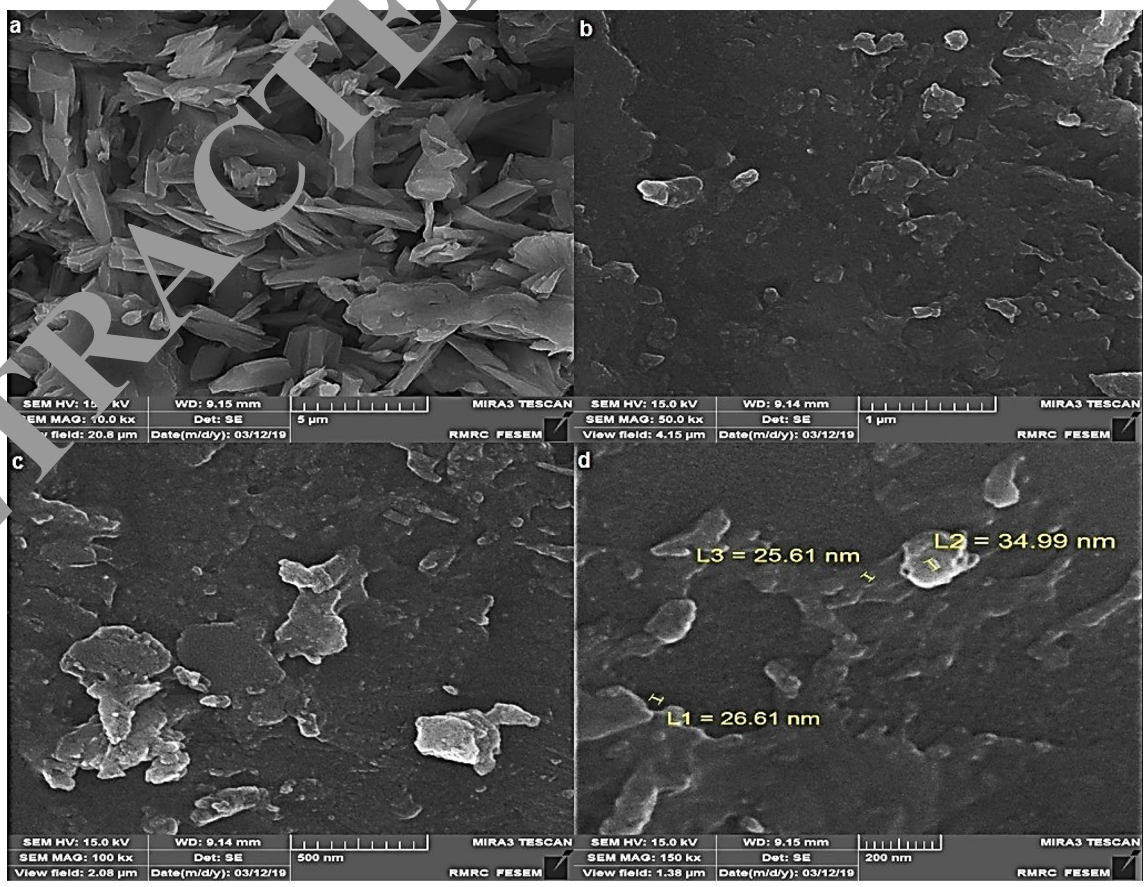

Figure 6. SEM images of CoNPs.

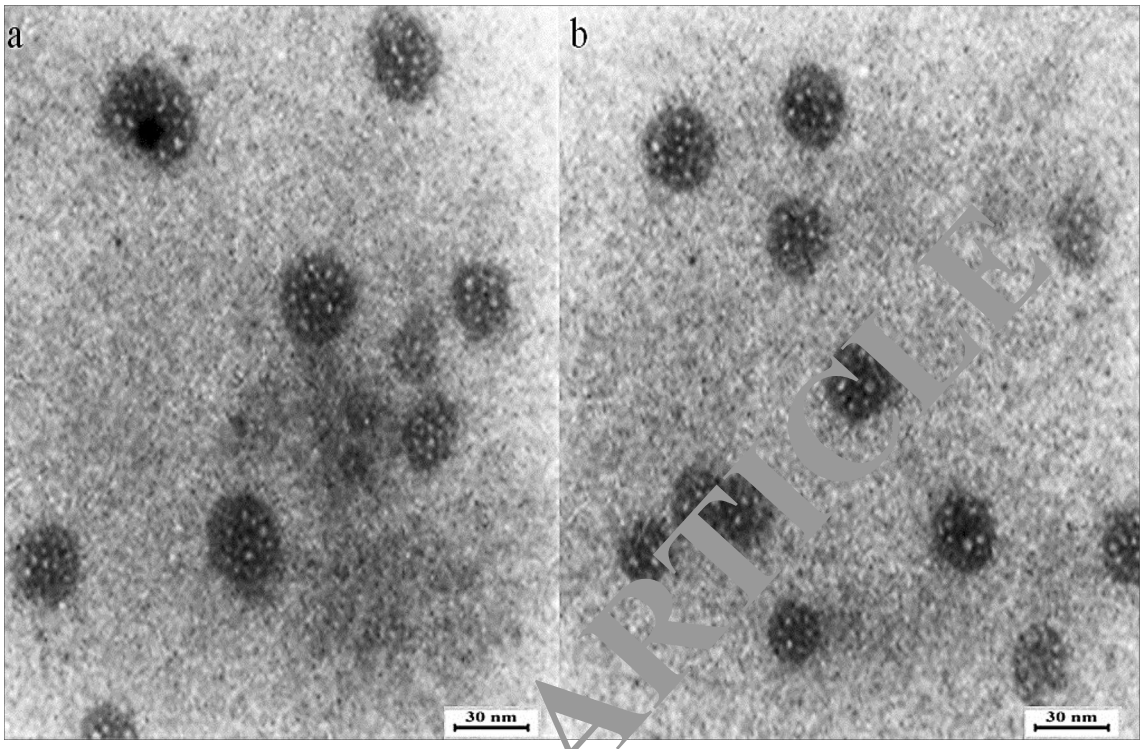

Figure 7. TEM images of CoNPs.

aggregated and make particles with large size. The aggregation of the nanoparticles is a well-known occurrence in biosynthesis methods of metallic nanoparticles, as it has been reported previously[45,46].

TEM analysis. TEM micrograph showed the surface morphology of synthesized nanoparticles (Fig. 7). The particle size distribution in the TEM image shows that the majority of nanoparticles were less than 30 nm. The particles were also found to be spherical. The SEM and TEM investigation gave similar results for the range of nanoparticles size. According our study, a few studies reported the biosynthesize of CoNPs using plants extracts. The range size of cobalt ferrites nanoparticles synthesized using aqueous extracts of sesame was 3–20.45 nm[47]. CoNPs was also biosynthesized using methanolic extracts of *Conocarpus erectus* and *Nerium indicum*. The size of particles was estimated in the range of 20–60 nm[37]. The average particle size of CoNPs, which was produced using aqueous extracts of *Raphanus sativus*, was reported 80 nm[36]. The particle size ranging from 20 to 50 nm was reported for of cobalt nanoparticles that were biosynthesized using *Moringa oleifera* extract[48].

EDS analysis. The EDS analysis of CoNPs is shown in Fig. 8. The result demonstrates the clear elemental composition profile of the biosynthesized CoNPs. The presences of cobalt in synthesized NPs was by the observed peaks including CoLα below of 1Kev; CoKα around 7Kev; and CoKβ below 8.

Antifungal and antibacterial effects of CoNPs. Analysis of results in this research (Tables 1, 2, 3, 4, 5, 6) revealed that almost all of the tested bacteria and fungi were sensitive to CoNPs and showed more antifungal and antibacterial activities than standard antibiotics. There was no significant difference in inhibitory zone of all bacteria between many dilutions of CoNPs and Difloxacin (30 mg/mL), Chloramphenicol (30), Streptomycin (10), Gentamicin (10), Oxytetracycline (30), Ampicillin (10), and Amikacin (25) and in inhibitory zone of all fungi between several concentrations of CoNPs and Fluconazole (60 mg/mL), Itraconazole (60), Miconazole (60), Amphotericin B (60), Nystatin (60). There was an increase in the inhibition zone in many of the samples when CoNPs increased. The findings showed a noticeable difference regarding sensitivity to CoNPs in the bacteria and fungi tested. The widest inhibition zone in agar well and disk diffusion test was seen at 64 mg/mL concentration. In agar well diffusion, no inhibitory effect of CoNPs was observed at 1 mg/mL concentration in the case of *E. coli* and *S. typhimurium* ($p \leq 0.01$). CoNPs prevented *B. subtilis*, *S. pneumonia*/*S. aureus*/*P. aeruginosa*/*C. glabrata*/*C. guilliermondii*/*C. krusei*, and *E. coli*/*S. typhimurium*/*C. albicans* growth at 1, 2, and 4 mg/mL concentrations, respectively and destroyed *B. subtilis*/*S. pneumonia*/*S. aureus*/*P. aeruginosa*/*C. krusei*, *E. coli*/*C. guilliermondii*/*C. glabrata*/*C. albicans*, and *S. typhimurium* at 2, 4, and 8 mg/mL concentrations, respectively. Thus, the findings showed strong antifungal and antibacterial properties of CoNPs against all of the tested fungi and bacteria. Moreover, CoNPs had the highest antibacterial and antifungal effects on *B. subtilis* and *C. krusei*, respectively ($p \leq 0.01$). In agreement with our experiment, in study of Hemmati et al.[5] showed that metal nanoparticles had strong antibacterial activities against Gram-negative bacteria include *Proteus mirabilis* (ATCC No. 25933), *Shigella flexneri* (ATCC No. 12022), *Listeria monocytogenes* (ATCC No. 13932), *Klebsiella pneumonia* (ATCC No. 9997), *Pseudomonas aeruginosa* (ATCC No. 27853), *Escherichia coli* O157:H7 (ATCC

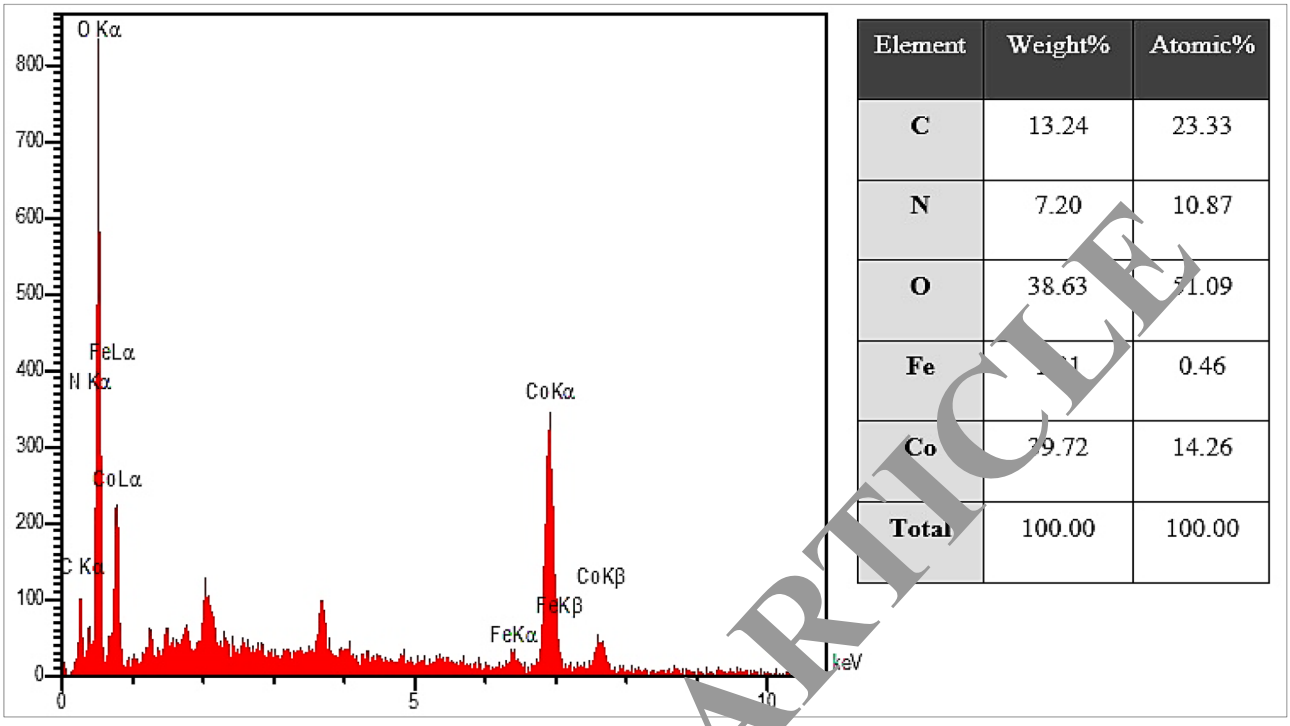

Element	Weight%	Atomic%
C	13.24	23.33
N	7.20	10.87
O	38.63	51.09
Fe	1.31	0.46
Co	39.72	14.26
Total	100.00	100.00

Figure 8. EDS analysis of CoNPs.

No. 25922), and *Salmonella typhimurium* (ATCC No. 14028) and Gram-positive bacteria include *Enterococcus faecalis* (ATCC No. 29212), *Bacillus subtilis* (ATCC No. 6633), *Streptococcus pyogenes* (ATCC No. 10403), *Staphylococcus saprophyticus* (ATCC No. 49453), *Staphylococcus epidermidis* (ATCC No. 12228), *Staphylococcus aureus* (ATCC No. 25923), and *Streptococcus pneumonia* (ATCC No. 49619)[5].

Cutaneous wound healing potential of CoNPs. In the recent experiment, the findings of wound area and contractures, total cell and blood vessel revealed that CoNPs ointment significantly ($p \leq 0.01$) amended the above parameters at day 10 compared to the other groups (Tables 7, 8; Figs. 9,10). Angiogenesis is defined as the formation of new capillaries from previous vessels. Angiogenesis is a controlled process that is rarely seen in adults except in instances of wound healing and menstrual cycle in women[49]. It is also a phenomenon that mostly occurs in impaired areas, which is aimed at secreting cytokines in the vessels to repair tissues. Angiogenesis is higher in the early days, reaching its maximum level from days 10 to 15. This level is then reduced with complete withdrawal of cytokines and other tissue repair factors[50].

In our study, CoNPs ointment increased significantly ($p \leq 0.01$) the number of fibrocyte, the concentration of hydroxyproline, hexuronic acid, and hexosamine and fibrocyte/fibroblast ratio at day 10 compared to the other groups (Tables 8, 9; Fig. 11). Fibroblasts are removed through the blood vessels formed at the wound site and are developed into fibrocytes after some time. The amount of fibroblast is usually high until day ten. The main role of fibroblasts is making collagen. In fact, fibroblasts synthesize collagen, repair the external matrix, and facilitate the wound contraction process[51]. One of the methods of wound healing facilitation is the use of fibroblast growth stimulant. It has been found that increasing the number of fibroblasts in the artificial skin leads to wound healing in in-vitro conditions[52]. Fibroblasts synthesize some components of the primary extracellular matrix of the wound bed such as fibronectin, hexosamine, and hexuronic acid, which provides a favorable ground for cell migration and proliferation. Fibroblasts then synthesize collagen, which provides tensile strength in the wound bed[53]. Fibrocytes are developed fibroblasts that have a higher ability in making collagen than fibroblasts. The more is the number of fibroblasts, the better is the wound healing[51]. Collagens are protein strains that are made of glycine, praline, and hydroxy proline amino acids. The amount of collagen is very low in the early days but abundantly found in the final days due to the increased number of fibroblasts. The tensile strength of wound is dependent not only on the content of tissue collagen but also on the organization and arrangement of collagen fibers and maturity of fibers[53].

The results of analysis of inflammatory cells (lymphocyte, macrophage, and neutrophil) indicated that CoNPs ointment regulated significantly ($p \leq 0.01$) the number of these cells at day 10 compared to the other groups (Table 8). Lymphocytes, existing in the human peripheral blood mononuclear cells, are an important source of immunoregulatory cytokines in the blood circulation and inflammatory parts of the body. Lymphocytes are increased in the early days[54]. Macrophages are the most important cells in the inflammatory stage that contribute to the elimination of necrotic tissues and bacteria[55]. These cells also contribute to the localization of inflammation process and absorption of fibroblasts to initiate proliferation by releasing some chemotoxic factors. Therefore, any factor that absorbs or activates the macrophages may have a positive impact on the repair process. In the absence

Dilution (mg/mL)	Inhibition zone in disk diffusion (mm)			
	C. albicans	*C. glabrata*	*C. guilliermondii*	*C. krusei*
Fluconazole (60)	39 ± 0.7^{a}	42.4 ± 1.34^{a}	45 ± 1^{a}	44.2 ± 1.3^{a}
Itraconazole (60)	35.6 ± 0.89^{ab}	40.4 ± 0.89^{a}	43.4 ± 0.89^{a}	41.4 ± 0.54^{a}
Miconazole (60)	41.6 ± 0.89^{a}	45.2 ± 1.3^{a}	46.2 ± 1.3^{a}	40.4 ± 1.34^{a}
Amphotericin B (60)	36.4 ± 0.89^{ab}	41.4 ± 1.34^{a}	40.2 ± 0.83^{a}	38.6 ± 0.89^{a}
Nystatin (60)	31.2 ± 1.3^{ab}	37.2 ± 1.3^{ab}	40.8 ± 0.44^{a}	35.4 ± 0.89^{ab}
CoNPs (64)	41.4 ± 1.34^{a}	43.2 ± 0.83^{a}	44.6 ± 0.89^{a}	44.2 ± 1.3^{a}
CoNPs (32)	35.4 ± 1.34^{ab}	40.2 ± 1.3^{a}	39.2 ± 0.83^{a}	40.6 ± 1.14^{a}
CoNPs (16)	31.6 ± 0.89^{ab}	33.8 ± 1.09^{ab}	35.4 ± 0.54^{ab}	35.2 ± 0.83^{ab}
CoNPs (8)	24.2 ± 1.3^{b}	28.6 ± 0.89^{b}	31.4 ± 1.34^{ab}	32.2 ± 1.3^{ab}
CoNPs (4)	21.2 ± 0.44^{bc}	23.4 ± 0.89^{b}	25.2 ± 1.3^{b}	28.8 ± 0.44^{b}
CoNPs (2)	16.6 ± 0.89^{bc}	19.2 ± 1.3^{bc}	21.2 ± 0.44^{bc}	22.6 ± 0.89^{bc}
CoNPs (1)	13.2 ± 0.83^{c}	17.6 ± 1.14^{bc}	18.2 ± 0.83^{bc}	16.2 ± 0.44^{bc}
Z. clinopodioides (64)	32 ± 1.22^{ab}	35.2 ± 1.3^{ab}	34 ± 1.22^{ab}	35.2 ± 1.3^{ab}
Z. clinopodioides (32)	30.4 ± 0.89^{ab}	31.4 ± 1.34^{ab}	29.4 ± 1.34^{b}	31.4 ± 1.34^{ab}
Z. clinopodioides (16)	24.4 ± 1.34^{b}	25.2 ± 0.44^{b}	24 ± 0.7^{b}	25 ± 0.7^{b}
Z. clinopodioides (8)	21 ± 1^{bc}	21.2 ± 1.3^{bc}	21.6 ± 0.89^{bc}	$2.4 \pm$ [illegible] ^{bc}
Z. clinopodioides (4)	15.2 ± 1.3^{bc}	20.2 ± 0.83^{bc}	19.4 ± 0.89^{bc}	17.4 ± 1.34
Z. clinopodioides (2)	12.2 ± 0.83^{c}	16.2 ± 0.83^{bc}	16.8 ± 0.44^{bc}	17.6 ± 0.89^{bc}
Z. clinopodioides (1)	11.4 ± 1.34^{c}	11.6 ± 0.89^{c}	13.2 ± 1.3^{c}	[illegible] ^{c}
$Co(NO_3)_2$ (64)	25.6 ± 0.89^{b}	28.6 ± 0.89^{b}	29.2 ± 0.83^{b}	[illegible] ^{b}
$Co(NO_3)_2$ (32)	24.8 ± 0.44^{b}	22 ± 1.22^{bc}	$24.4 \pm$	24.8 ± 1.09^{b}
$Co(NO_3)_2$ (16)	21.2 ± 1.3^{bc}	18.4 ± 0.89^{bc}	21.2 ± 1.3^{bc}	19.6 ± 0.89^{bc}
$Co(NO_3)_2$ (8)	15.4 ± 0.54^{bc}	16 ± 0.7^{bc}	16.6 ± 1.1 [illegible] ^{bc}	16.6 ± 1.14^{bc}
$Co(NO_3)_2$ (4)	10.4 ± 1.34^{c}	$13.8 \pm$	12 ± 1^{c}	14.2 ± 1.3^{c}
$Co(NO_3)_2$ (2)	9 ± 0^{c}	[illegible] $\pm 0.89^{c}$	1.6 ± 1.14^{c}	11 ± 0^{c}
$Co(NO_3)_2$ (1)	0 ± 0^{d}	$0 \pm$	0 ± 0^{d}	8 ± 0^{c}
Distilled water	0 ± 0^{d}	0 ± 0^{d}	0 ± 0^{d}	0 ± 0^{d}

Table 1. The growth inhibition zones of fungi in agar disk diffusion assay in various concentrations of CoNPs, *Z. clinopodioides*, and $Co(NO_3)_2$. Non-identical letters reveal a notable shift between the experimental groups ($p \leq 0.01$).

of macrophages, the number of fibroblasts migrating to the wound is also reduced[56]. Stimulation of receptors on the surface of cutaneous macrophages stimulates these cells to produce cytokines and advance some stages of wound healing[54,56]. Neutrophils prepare the wound area for tissue regeneration by cleaning the wound site from infection and microorganisms. These cells contribute to the acceleration of inflammatory response by releasing some chemotoxic factors to absorb other leucocytes[13]. Accumulation and overactivation of lymphocytes, macrophages, and neutrophils in the wound site and their extreme secretion produce pus in the infection site, which reduces the wound healing process and may lead to complete loss of the impaired tissue and even amputation. Further, the presence of free radicals in the wound site may increase the amount of pus[57,58].

Antioxidant activity of CoNPs. DPPH free radical scavenging effect of *Z. clinopodioides* and CoNPs in several concentrations (0, 1, 3, 7, 15, 31, 62, 125, 250, 500, and 1000 µg/mL) indicated impressive prevention similar to BHT. The IC50 of *Z. clinopodioides*, BHT, and CoNPs were 448, 342, and 342 µg/mL, respectively (Fig. 12). Agreement with our experiment, in the previous studies, indicated that metal nanoparticles had strong antioxidant properties, and they destroyed several free radicals such as DPPH[4,5].

Antioxidant compounds reduce the free radicals and pus in the wound area, thereby healing the wound completely[59,60]. Other papers have reported that the medicinal plants and their extraction rich in anti-inflammatory and antioxidant compounds significantly decrease the production of pus and enhance the wound healing process[59,60]. Our study indicated that CoNPs had a strong antioxidant activity. Therefore, it was normal to observe that CoNPs ointment had a notable wound healing activity.

Cytotoxicity survey of CoNPs. The cells treated with various concentrations of the present $Co(NO_3)_2$, *Z. clinopodioides*, and CoNPs were examined by MTT test for 48 h regarding cytotoxic effects on HUVEC cells. The absorbance rate was determined at 570 nm, which indicated extraordinary viability on HUVEC line even up to 1000 µg/mL for $Co(NO_3)_2$, *Z. clinopodioides*, and CoNPs (Fig. 13). The absence of any significant toxicity of CoNPs has numerous safe applications in pharmaceutical domains. Agreement with our experiment, in the study of Hamelian et al.[4] revealed when metal salts combine with biological compounds, their cytotoxicity removed[4].

Dilution (mg/mL)	Inhibition zone in well diffusion (mm)			
	C. albicans	*C. glabrate*	*C. guilliermondii*	*C. krusei*
CoNPs (64)	30.6 ± 0.89^{a}	34.6 ± 1.14^{a}	34.2 ± 0.44^{a}	35.4 ± 0.54^{a}
CoNPs (32)	25 ± 1^{ab}	31.2 ± 0.83^{a}	31.2 ± 1.3^{a}	32.8 ± 0.44^{a}
CoNPs (16)	19.4 ± 0.89^{bc}	27.2 ± 1.3^{ab}	25.4 ± 0.54^{ab}	26.2 ± 1.3^{ab}
CoNPs (8)	14.2 ± 1.3^{c}	25.2 ± 1.3^{ab}	21 ± 1.22^{b}	23.4 ± 1.34^{b}
CoNPs (4)	11.4 ± 0.54^{c}	21.4 ± 1.34^{b}	20.6 ± 0.89^{b}	20.2 ± 1.3^{b}
CoNPs (2)	8.2 ± 1.3^{c}	15.4 ± 0.89^{bc}	15.8 ± 1.09^{bc}	17.2 ± 0.83^{bc}
CoNPs (1)	8.2 ± 0.44^{c}	11.6 ± 0.89^{c}	12.8 ± 0.44^{c}	13.4 ± 0.89^{c}
Z. clinopodioides (64)	19.8 ± 0.44^{bc}	21.6 ± 0.89^{b}	23.2 ± 1.3^{b}	25.6 ± 1.14^{ab}
Z. clinopodioides (32)	15.6 ± 0.89^{bc}	17.4 ± 1.34^{bc}	20 ± 0^{b}	22.2 ± 1.3^{b}
Z. clinopodioides (16)	13.6 ± 1.14^{c}	14.6 ± 1.14^{c}	14.2 ± 0.44^{c}	21.4 ± 1.34^{b}
Z. clinopodioides (8)	11.4 ± 1.34^{c}	12.4 ± 0.89^{c}	13 ± 1^{c}	14.6 ± 0.89^{c}
Z. clinopodioides (4)	9.4 ± 1.34^{c}	9.6 ± 0.89^{c}	11.2 ± 1.3^{c}	12.4 ± 0.54^{c}
Z. clinopodioides (2)	0 ± 0^{d}	9.4 ± 0.54^{c}	10 ± 1.22^{c}	11.6 ± 0.89^{c}
Z. clinopodioides (1)	0 ± 0^{d}	0 ± 0^{d}	0 ± 0^{d}	0 ± 0^{d}
$Co(NO_3)_2$ (64)	13.2 ± 0.83^{c}	16.8 ± 1.09^{bc}	18 ± 1^{bc}	19 ± 0.7^{bc}
$Co(NO_3)_2$ (32)	11.6 ± 0.89^{c}	14.8 ± 0.44^{c}	13.6 ± 0.89^{c}	15 ± 1^{bc}
$Co(NO_3)_2$ (16)	9.8 ± 0.44^{c}	12.4 ± 1.34^{c}	12.4 ± 1.34^{c}	13.8 ± 1.09
$Co(NO_3)_2$ (8)	9.4 ± 0.89^{c}	11.2 ± 1.3^{c}	12.6 ± 0.89^{c}	11.2 ± 1.3^{c}
$Co(NO_3)_2$ (4)	0 ± 0^{d}	10.6 ± 0.89^{c}	9.8 ± 0.44^{c}	10 ± 0^{c}
$Co(NO_3)_2$ (2)	0 ± 0^{d}	0 ± 0^{d}	0 ± 0^{d}	0 ± 0^{d}
$Co(NO_3)_2$ (1)	0 ± 0^{d}	0 ± 0^{d}	0 ± 0^{d}	0 ± 0^{d}
Distilled water	0 ± 0^{d}	0 ± 0^{d}	0 ± 0^{d}	0 ± 0^{d}

Table 2. The growth inhibition zones of fungi in agar well diffusion assay in various concentrations of CoNPs, *Z. clinopodioides*, and $Co(NO_3)_2$. Non-identical letters reveal a notable shift between the experimental groups ($p \leq 0.01$).

Dilution (mg/mL)	*C. albicans*	*C. glabrata*	*C. guilliermondii*	*C. krusei*
MIC_{CoNPs}	4 ± 0^{A}	2 ± 0^{A}	2 ± 0^{a}	2 ± 0^{a}
$MIC_{Z.\ clinopodioides}$	8 ± 0^{c}	4 ± 0^{b}	4 ± 0^{b}	4 ± 0^{b}
$MIC_{Co(NO3)2}$	8 ± 0^{c}	8 ± 0^{c}	4 ± 0^{c}	2 ± 0^{c}
MFC_{CoNPs}	4 ± 0^{B}	4 ± 0^{B}	4 ± 0^{B}	2 ± 0^{A}
$MFC_{Z.\ clinopodioides}$	8 ± 0^{C}	8 ± 0^{C}	8 ± 0^{C}	4 ± 0^{C}
$MFC_{Co(NO_3)_2}$	16 ± 0^{D}	8 ± 0^{D}	8 ± 0^{D}	8 ± 0^{D}

Table 3. MIC and MFC of CoNPs, *Z. clinopodioides*, and $Co(NO_3)_2$ against fungi. Non-identical letters reveal a notable shift between the experimental groups ($p \leq 0.01$).

Enzyme results. *Cholinesterase enzymes inhibition results.* All of novel nanoparticles (CoNPs) had remarkably higher AChE inhibitory effect than of control AChE inhibitor compound such as Tacrine. Indeed, the Ki values of novel nanoparticles and standard compound (tacrine) are summarized in Table 2. High inhibitory effect on ACHe (of these new nanoparticles), with Ki values of 0.42 ± 0.11 and 1.04 ± 0.24 mM. Later, all of these new nanoparticles obtained at the end of the experiment showed close inhibition profiles. The most active $Co(NO_3)_2$ showed Ki value of 0.42 ± 0.11 mM. The IC50 values of TAC as positive control for AChE and new nanoparticles were examined in the following order: $Co(NO_3)_2$ (0.68 mM, r^2: 0.9654) < CoNPs (1.24 mM, r^2: 0.9139) < TAC (1.98 mM, r^2: 0.9883). The IC50 values of TAC as positive control for BChE and new nanoparticles are in the following order: $Co(NO_3)_2$ (1.32 mM, r^2: 0.9768) < CoNPs (2.20 mM, r^2: 0.9861) < TAC (3.84 mM, r^2: 0.9812). In addition, new nanoparticles effectively inhibited BChE with values of 1.18 ± 0.17 and 1.91 ± 0.38 mM Ki, respectively. At the same time, all of these new nanoparticles synthesized had nearly close inhibition profiles. The most active $Co(NO_3)_2$ effectively inhibited BChE, with Ki value of 1.18 ± 0.17 mM. Indeed, recording novel inhibitors targeting AChE has still been of significant interest to the researchers. Additionally, it is recorded that selective BChE inhibitors can circumvent classical cholinergic toxicity. Hence, the development of novel selective BChE inhibitor compounds can provide additional benefits in the therapy of AD[61].

Dilution (mg/mL)	Inhibition zone in disk diffusion (mm)					
	Gram-positive bacteria			Gram-negative bacteria		
	S. typhimurium	*E. coli*	*P. aeruginosa*	*S. aureus*	*S. pneumoniae*	*B. subtilis*
Difloxacin (30)	27 ± 0.7^{b}	29.2 ± 0.44^{b}	33.8 ± 1.09^{ab}	27.2 ± 1.3^{b}	24.2 ± 0.44^{b}	30.6 ± 0.89^{ab}
Chloramphenicol (30)	25.6 ± 0.89^{b}	22.4 ± 0.54^{bc}	23.6 ± 1.14^{b}	23.4 ± 0.89^{b}	24.2 ± 0.83^{b}	27 ± 0.7^{b}
Streptomycin (10)	17.2 ± 1.3^{bc}	20.2 ± 0.83^{bc}	17.2 ± 1.3^{bc}	17.6 ± 0.89^{bc}	18.2 ± 1.3^{bc}	28.2 ± 1.3^{b}
Gentamicin (10)	20.4 ± 1.34^{bc}	25.4 ± 1.34^{b}	20.8 ± 1.09^{bc}	20 ± 1.22^{bc}	22.4 ± 0.89^{bc}	21 ± 1^{bc}
Oxytetracycline (30)	26.4 ± 0.54^{b}	24 ± 1^{b}	20.2 ± 1.3^{bc}	24.6 ± 0.89^{b}	23.2 ± 1.3^{b}	24.4 ± 0.54^{b}
Ampicillin (10)	19.2 ± 1.3^{bc}	24.4 ± 1.34^{b}	19.2 ± 1.3^{bc}	24 ± 0.7^{b}	20.8 ± 0.44^{bc}	[illegible]
Amikacin (25)	28.2 ± 0.83^{b}	24.2 ± 1.3^{b}	21.6 ± 1.14^{bc}	25.6 ± 0.89^{b}	27.6 ± 1.14^{b}	[illegible]
CoNPs (64)	40.6 ± 1.14^{a}	41.8 ± 0.44^{a}	45.2 ± 0.44^{a}	44.2 ± 0.44^{a}	46.2 ± 1.3^{a}	[illegible]
CoNPs (32)	33.4 ± 1.34^{ab}	36.4 ± 0.89^{ab}	38.6 ± 0.89^{a}	38.2 ± 1.3^{a}	[illegible]	[illegible]
CoNPs (16)	28 ± 1.22^{b}	34.4 ± 1.34^{ab}	32.2 ± 0.83^{ab}	34.4 ± 1.34^{ab}	[illegible]	[illegible]
CoNPs (8)	24 ± 1.22^{b}	26.2 ± 1.3^{b}	30.2 ± 1.3^{ab}	30 ± 1.22^{ab}	[illegible]	29.4 ± 0.89^{b}
CoNPs (4)	21.4 ± 0.54^{bc}	21 ± 0.7^{bc}	25 ± 1.22^{b}	24 ± 1^{b}	[illegible]	23.2 ± 1.3^{b}
CoNPs (2)	15.2 ± 1.3^{bc}	14.4 ± 0.89^{c}	21.4 ± 0.89^{bc}	[illegible]	21 ± 0.7^{bc}	20 ± 0.7^{bc}
CoNPs (1)	11.6 ± 1.14^{c}	11.4 ± 1.34^{c}	14.2 ± 0.83^{c}	[illegible]	[illegible]	17.6 ± 0.89^{bc}
Z. clinopodioides (64)	28 ± 1.22^{b}	29.6 ± 0.89^{b}	32.4 ± 1.34^{ab}	[illegible]	35 ± 0.7^{ab}	35 ± 0.7^{ab}
Z. clinopodioides (32)	24.2 ± 0.83^{b}	24.2 ± 1.3^{b}	26.4 ± 0.54^{b}	[illegible]	33.6 ± 1.14^{ab}	31.4 ± 1.34^{ab}
Z. clinopodioides (16)	21.4 ± 1.34^{bc}	22.2 ± 0.83^{bc}	[illegible]	24.6 ± 0.89^{b}	27.2 ± 1.3^{b}	27 ± 0.7^{b}
Z. clinopodioides (8)	15 ± 1^{bc}	17.8 ± 0.44^{bc}	[illegible]	[illegible]	24.4 ± 0.89^{b}	21.4 ± 0.54^{bc}
Z. clinopodioides (4)	11.2 ± 1.3^{c}	12.6 ± 1.14^{c}	14 ± 0^{c}	[illegible]	18.4 ± 0.54^{bc}	17.2 ± 1.3^{bc}
Z. clinopodioides (2)	9.2 ± 0.83^{c}	10.6 ± 0.89^{c}	[illegible]	12.2 ± 1.3^{c}	12 ± 1.22^{c}	14.8 ± 1.09^{c}
Z. clinopodioides (1)	0 ± 0^{d}	0 ± 0^{d}	[illegible]	8.8 ± 0.44^{c}	10.6 ± 0.89^{c}	11.8 ± 0.44^{c}
$Co(NO_3)_2$ (64)	22 ± 1.22^{bc}	24.8 ± 0.44^{b}	[illegible]	25 ± 1^{b}	27.6 ± 0.89^{b}	27.4 ± 1.34^{b}
$Co(NO_3)_2$ (32)	15.8 ± 1.09^{bc}	[illegible]	20 ± 0.7^{bc}	20.8 ± 0.44^{bc}	23.8 ± 1.09^{b}	23 ± 1.22^{b}
$Co(NO_3)_2$ (16)	12.2 ± 1.3^{c}	[illegible]	16.6 ± 0.89^{bc}	18 ± 0.7^{bc}	19.2 ± 1.3^{bc}	19.4 ± 1.34^{bc}
$Co(NO_3)_2$ (8)	9.4 ± 1.34^{c}	[illegible]	13 ± 1.22^{c}	14.4 ± 1.34^{c}	15 ± 0.7^{bc}	16.4 ± 0.54^{bc}
$Co(NO_3)_2$ (4)	8.4 ± 1.34^{c}	[illegible]	10 ± 0^{c}	11.4 ± 0.54^{c}	11.6 ± 0.89^{c}	13 ± 0^{c}
$Co(NO_3)_2$ (2)	[illegible]	[illegible]	0 ± 0^{d}	0 ± 0^{d}	8.8 ± 0.44^{c}	10.2 ± 1.3^{c}
$Co(NO_3)_2$ (1)	0 ± 0^{d}	0 ± 0^{d}	0 ± 0^{d}	0 ± 0^{d}	0 ± 0^{d}	0 ± 0^{d}
Distilled water	[illegible]	0 ± 0^{d}	0 ± 0^{d}	0 ± 0^{d}	0 ± 0^{d}	0 ± 0^{d}

Table 4. The growth inhibition zones of bacteria in agar disk diffusion assay in various concentrations of CoNPs, *Z. clinopodioides*, and $Co(NO_3)_2$. Non-identical letters reveal a notable shift between the experimental groups ($p \leq$ [illegible]).

Glycosidase inhibition results. For enzyme glycosidase, new nanoparticles (CoNPs) have IC50 values of 15.86 and 11.26 µM and Ki values of 18.51 ± 2.73 and 15.70 ± 3.10 mM (Table 10). The results obtained clearly showed that all of these novel compounds synthesized record the inhibitory effects of acarbose (IC50: 19.32 mM), which acts as a control glycosidase inhibitor. Indeed, the most effective Ki value of CoNPs was 15.70 ± 3.10 mM, respectively. For this metabolic enzyme, IC50 values of ACR as control and novel nanoparticles the following order: CoNPs (11.26 mM, r^2: 0.9371) < $Co(NO_3)_2$ (15.86 mM, r^2: 0.9760) < ACR (19.32 mM, r^2: 0.9646). Anti-diabetic drugs that are used in clinical practice, such as acarbose, voglibose and miglitol, competitively inhibit α-glucosidase in brush border of small intestine which subsequently interrupt hydrolysis of carbohydrate and improve postprandial hyperglycemia[62].

Conclusions

The recent research indicated an ecofriendly, clean and useful method to synthesize cobalt nanoparticles using *Z. clinopodioides* aqueous extract, in which no chemical substance was used. Due to the existing major problems in the physical and chemical methods for producing nanoparticles, there is a need to easy, low-cost, and non-toxic procedures. FT-IR, UV–Vis spectroscopy, EDS, and FESEM techniques were used to characterize CoNPs synthesized. The synthesized CoNPs have great antioxidant, antifungal, antibacterial, and cutaneous wound healing potentials. Also, the absence of any notable toxicity is another advantage that was evaluated and confirmed by the recent study. After confirming in the clinical trial sutides, this formulation can be used for the treatment of several types of cutaneous wounds in humans.

Dilution (mg/mL)	Inhibition zone in well diffusion (mm)					
	Gram-positive bacteria			Gram-negative bacteria		
	S. typhimurium	*E. coli*	*P. aeruginosa*	*S. aureus*	*S. pneumoniae*	*B. subtilis*
CoNPs (64)	33.6 ± 1.14^{ab}	36.2 ± 0.83^{a}	38.4 ± 0.54^{a}	38.2 ± 0.44^{a}	39 ± 1^{a}	40.2 ± 1.3^{a}
CoNPs (32)	31.4 ± 0.89^{ab}	31.2 ± 0.44^{ab}	31.4 ± 0.89^{ab}	31 ± 1^{ab}	34.6 ± 0.89^{ab}	33.8 ± 0.44^{ab}
CoNPs (16)	24.2 ± 1.3^{b}	26.2 ± 0.83^{b}	26.2 ± 1.3^{b}	27.4 ± 0.89^{b}	25.6 ± 1.14^{b}	29.4 ± 0.54^{b}
CoNPs (8)	20.6 ± 0.89^{bc}	22.4 ± 1.34^{bc}	21.4 ± 1.34^{bc}	24.4 ± 0.89^{b}	22.6 ± 0.89^{bc}	27.4 ± 0.89^{b}
CoNPs (4)	13.4 ± 1.34^{c}	15.6 ± 0.89^{bc}	17.2 ± 1.3^{bc}	18 ± 1.22^{bc}	18.4 ± 0.54^{bc}	21.2 ± 1.3^{bc}
CoNPs (2)	8.2 ± 0.44^{c}	10.4 ± 0.54^{c}	12 ± 0^{c}	14.2 ± 0.44^{c}	13.2 ± 1.3^{c}	15.2 ± 0.8^{c}
CoNPs (1)	0 ± 0^{d}	0 ± 0^{d}	8.4 ± 1.34^{c}	9.8 ± 0.44^{c}	10.4 ± 0.54^{c}	12.2 ± 0.8^{c}
Z. clinopodioides (64)	24.8 ± 0.44^{b}	25.4 ± 0.89^{b}	27 ± 1^{b}	28.8 ± 0.44^{b}	28.4 ± 0.89^{b}	30.8 ± 1.09^{ab}
Z. clinopodioides (32)	19.6 ± 1.14^{bc}	21.2 ± 1.3^{bc}	23.8 ± 0.44^{b}	24 ± 0.7^{b}	22.8 ± 0.44^{bc}	27.2 ± 0.44^{b}
Z. clinopodioides (16)	13.2 ± 0.83^{c}	19 ± 1.22^{bc}	20.8 ± 1.09^{bc}	19.2 ± 0.83^{bc}	20.4 ± 0.54^{bc}	24.4 ± 1.34^{bc}
Z. clinopodioides (8)	11.8 ± 1.09^{c}	13 ± 1^{c}	15.8 ± 1.09^{bc}	14 ± 1.22^{c}	17 ± 1^{bc}	16 ± 1.22^{bc}
Z. clinopodioides (4)	8.2 ± 0.83^{c}	9.2 ± 1.3^{c}	10.4 ± 1.34^{c}	12 ± 0.7^{c}	13.2 ± 1.14^{c}	15.4 ± 1.34^{bc}
Z. clinopodioides (2)	0 ± 0^{d}	8.2 ± 0.44^{c}	10.6 ± 1.14^{c}	9.6 ± 0.89^{c}	10 ± 0.7^{c}	12 ± 1.22^{c}
Z. clinopodioides (1)	0 ± 0^{d}	0 ± 0^{d}	0 ± 0^{d}	0 ± 0^{d}	0 ± 0^{d}	10 ± 0^{c}
$Co(NO_3)_2$ (64)	14.4 ± 0.54^{c}	16.4 ± 0.89^{bc}	18 ± 0.7^{bc}	17 ± 1^{bc}	18 ± 0.7^{bc}	20.6 ± 0.89^{bc}
$Co(NO_3)_2$ (32)	10.2 ± 1.3^{c}	11.6 ± 1.14^{c}	13 ± 0.7^{c}	13 ± 0^{c}	14.8 ± 0.44^{c}	17.8 ± 0.44^{bc}
$Co(NO_3)_2$ (16)	8.6 ± 0.89^{c}	9.2 ± 0.83^{c}	11.2 ± 1.3^{c}	12.4 ± 1.34^{c}	12.4 ± 0.54^{c}	13.2 ± 1.3^{c}
$Co(NO_3)_2$ (8)	0 ± 0^{d}	8 ± 0^{c}	10 ± 0^{c}	10.4 ± 0.89^{c}	11 ± 0.7^{c}	11 ± 0.7^{c}
$Co(NO_3)_2$ (4)	0 ± 0^{d}	0 ± 0^{d}	0 ± 0^{d}	0 ± 0^{d}	8.4 ± 0.54^{c}	9.8 ± 0.44^{c}
$Co(NO_3)_2$ (2)	0 ± 0^{d}	0 ± 0^{d}	0 ± 0^{d}	0 ± 0^{d}	0 ± 0^{d}	0 ± 0^{d}
$Co(NO_3)_2$ (1)	0 ± 0^{d}	0 ± 0^{d}	0 ± 0^{d}	0 ± 0^{d}	0 ± 0^{d}	0 ± 0^{d}
Distilled water	0 ± 0^{d}	0 ± 0^{d}	0 ± 0^{d}	0 ± 0^{d}	0 ± 0^{d}	0 ± 0^{d}

Table 5. The growth inhibition zones of bacteria in agar well diffusion assay in various concentrations of CoNPs, *Z. clinopodioides*, and $Co(NO_3)_2$. Non-identical letters reveal a notable shift between the experimental groups ($p \leq 0.01$).

Dilution (mg/mL)	Gram-negative bacteria			Gram-positive bacteria		
	S. typhimurium	*E. coli*	*P. aeruginosa*	*S. aureus*	*S. pneumoniae*	*B. subtilis*
MIC_{CoNPs}	4 ± 0^{c}	4 ± 0^{c}	2 ± 0^{b}	2 ± 0^{b}	2 ± 0^{b}	1 ± 0^{a}
$MIC_{Z.\ clinopodioid}$	8 ± 0^{d}	8 ± 0^{d}	8 ± 0^{d}	8 ± 0^{d}	4 ± 0^{c}	2 ± 0^{b}
$MIC_{Co(NO3)2}$	16 ± 0^{e}	8 ± 0^{d}	8 ± 0^{d}	8 ± 0^{d}	4 ± 0^{c}	4 ± 0^{c}
MBC_{C}	8 ± 0^{C}	4 ± 0^{B}	2 ± 0^{A}	2 ± 0^{A}	2 ± 0^{A}	2 ± 0^{A}
$MBC_{Z.\ clinopodioides}$	16 ± 0^{D}	16 ± 0^{D}	8 ± 0^{C}	8 ± 0^{C}	4 ± 0^{B}	4 ± 0^{B}
$MBC_{Co(NO3)2}$	32 ± 0^{E}	32 ± 0^{E}	8 ± 0^{C}	16 ± 0^{D}	8 ± 0^{C}	8 ± 0^{C}

Table 6. MIC and MBC of CoNPs, *Z. clinopodioides*, and $Co(NO_3)_2$ against bacteria. Non-identical letters reveal a notable shift between the experimental groups ($p \leq 0.01$).

Parameters	Groups (n = 10)					
	Control	Basal ointment	Tetracycline ointment	$Co(NO_3)_2$ ointment	*Z. clinopodioides* ointment	CoNPs ointment
Wound area (cm^2)	2.6 ± 0.2^{c}	2.6 ± 0.2^{c}	1.9 ± 0.1^{b}	2 ± 0^{b}	1.8 ± 0.3^{b}	1.2 ± 0.1^{a}
Wound contractures (%)	35 ± 4^{c}	35 ± 4^{c}	52.5 ± 2^{b}	50 ± 0^{b}	55 ± 6^{b}	70 ± 2^{a}

Table 7. The level of macroscopic parameters in experimental groups. Non-identical letters reveal a notable shift between the experimental groups ($p \leq 0.05$).

Parameters	Groups (n = 10)					
	Control	Basal ointment	Tetracycline ointment	$Co(NO_3)_2$ ointment	*Z. clinopodioides* ointment	CoNPs ointment
Total cell (n)	$1,398.9 \pm 32.8^{c}$	$1,376.2 \pm 24.3^{c}$	$1,210.1 \pm 32.1^{b}$	$1,254.6 \pm 25.4^{b}$	$1,232.9 \pm 19.6^{b}$	984.3 ± 32.1^{a}
Vessel (n)	3.8 ± 0.2^{c}	4.2 ± 0.4^{c}	7.9 ± 0.7^{b}	7.1 ± 0.5^{b}	7.9 ± 0.5^{b}	12.5 ± 0.4^{a}
Fibrocyte (n)	2.1 ± 0.1^{c}	2.5 ± 0.3^{c}	6.1 ± 0.4^{b}	5.4 ± 0.3^{b}	9.9 ± 0.4^{a}	11 ± 0.5^{a}
Fibroblast (n)	13.2 ± 0.8^{d}	14.3 ± 1.2^{d}	18.8 ± 0.7^{c}	23.3 ± 0.5^{b}	23.9 ± 0.2^{b}	27.9 ± 1.1^{a}
Fibrocyte to fibroblast (ratio)	0.15 ± 0.02^{d}	0.17 ± 0.01^{d}	0.32 ± 0.02^{b}	0.23 ± 0.02^{c}	0.41 ± 0.03^{a}	0.39 ± 0.02^{a}
Lymphocyte (n)	21.3 ± 0.9^{c}	19.9 ± 0.7^{c}	12.1 ± 0.5^{b}	13.5 ± 0.8^{b}	12.1 ± 0.7^{b}	6.4 ± 0.6^{a}
Macrophage (n)	4.8 ± 0.2^{a}	4.6 ± 0.4^{a}	5.1 ± 0.3^{a}	5.2 ± 0.4^{a}	4.5 ± 0.2^{a}	4.8 ± 0.5^{a}
Neutrophil (n)	32.5 ± 1.5^{d}	29.8 ± 0.9^{d}	15.6 ± 0.8^{b}	22.1 ± 0.9^{c}	$\pm 1.2^{b}$	4.5 ± 0.3^{a}

Table 8. The level of microscopic parameters in experimental groups. Non identical letters reveal a notable shift between the experimental groups ($p \leq 0.05$).

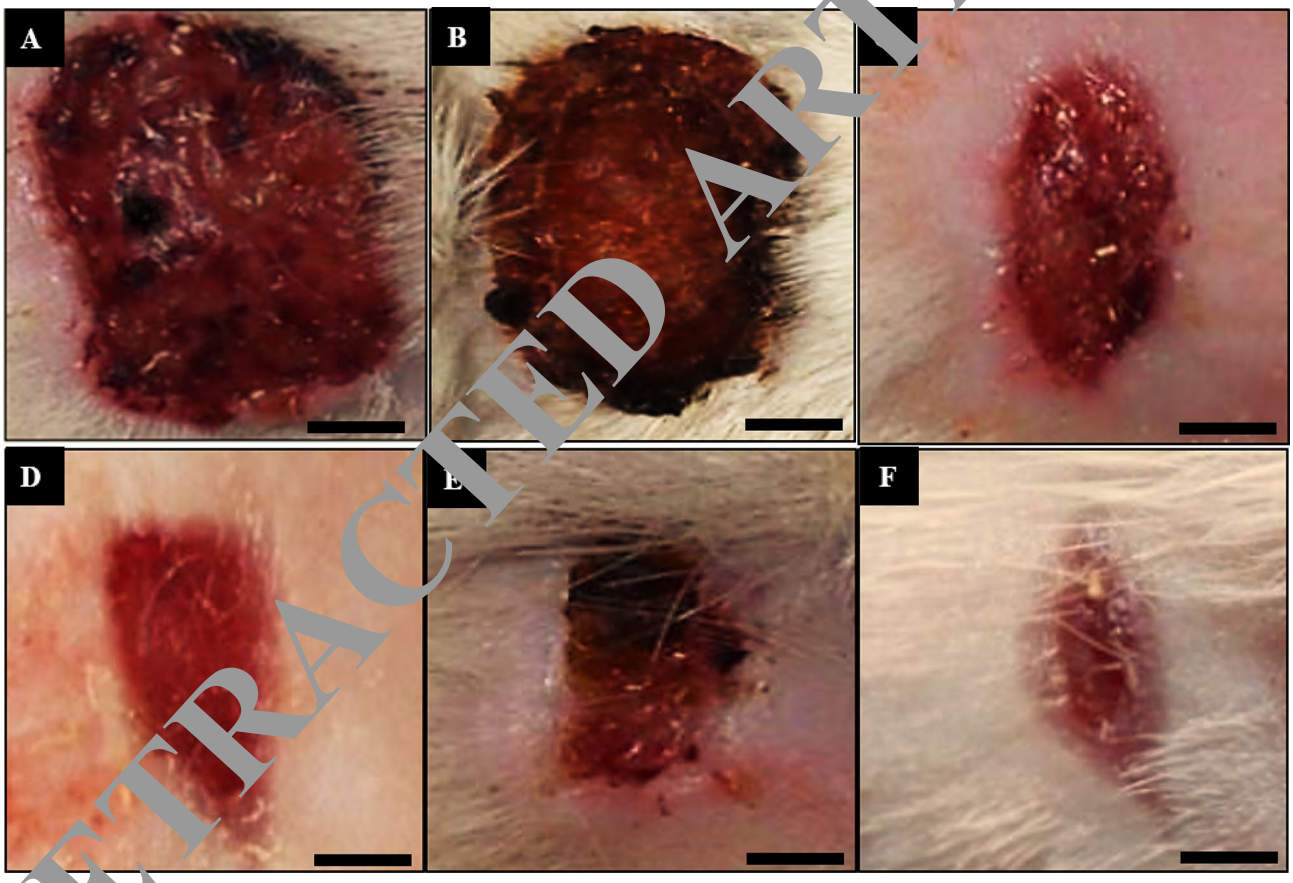

Figure 9. Macroscopic wound images of the control (**A**), basal ointment (**B**), tetracycline ointment (**C**), $Co(NO_3)_2$ ointment (**D**), *Z. clinopodioides* ointment (**E**), and CoNPs ointment (**F**) on 10 days post-injury. Scale bar: 4 mm.

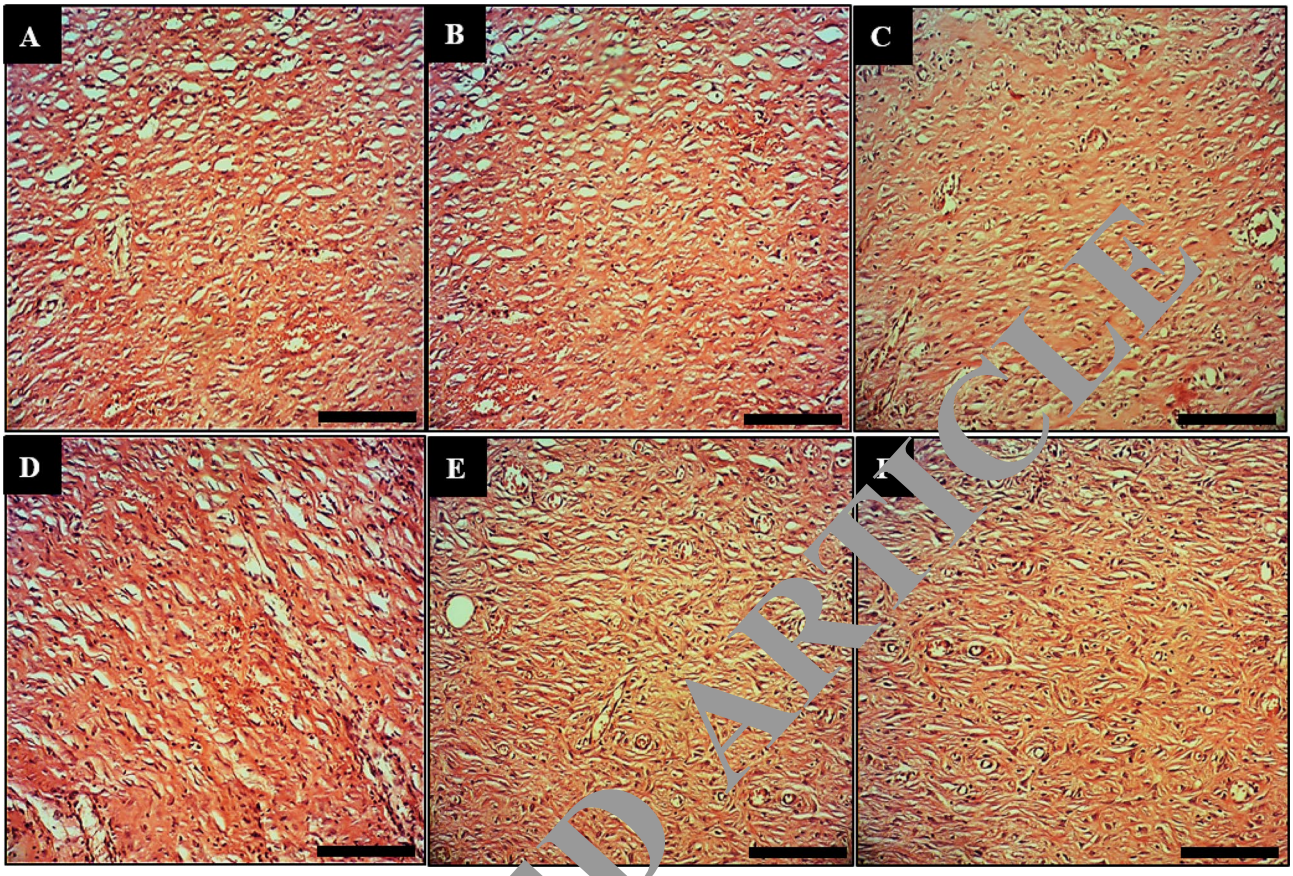

Figure 10. Longitudinal section of wounds of the control (**A**), basal ointment (**B**), tetracycline ointment (**C**), $Co(NO_3)_2$ ointment (**D**), *Z. clinopodioides* ointment (**E**), and CoNPs ointment (**F**) on 10 days post-injury. Scale bar: 150 µm. Magnification ×20.

Parameters	Groups (n = 10)					
	Control	Basal ointment	Tetracycline ointment	$Co(NO_3)_2$ ointment	*Z. clinopodioides* ointment	CoNPs ointment
Hydroxyproline (mg/g tissue)	12.4 ± 0.7^{d}	14.2 ± 0.9^{d}	25.1 ± 0.5^{b}	19.7 ± 1.1^{c}	27.5 ± 0.9^{b}	36.2 ± 0.9^{a}
Hexosamine (mg/100 mg of tissue)	0.21 ± 0.05^{c}	0.2 ± 0.04^{c}	0.31 ± 0.04^{b}	0.28 ± 0.01^{b}	0.32 ± 0.05^{b}	0.42 ± 0.05^{a}
Uronic acid (mg/100 mg of tissue)	0.11 ± 0.03^{c}	0.12 ± 0.03^{c}	0.19 ± 0.02^{b}	0.14 ± 0.02^{c}	0.21 ± 0.03^{b}	0.29 ± 0.04^{a}

Table 9. The level of biochemical parameters in experimental groups. Non-identical letters reveal a notable shift between the experimental groups ($p \leq 0.05$).

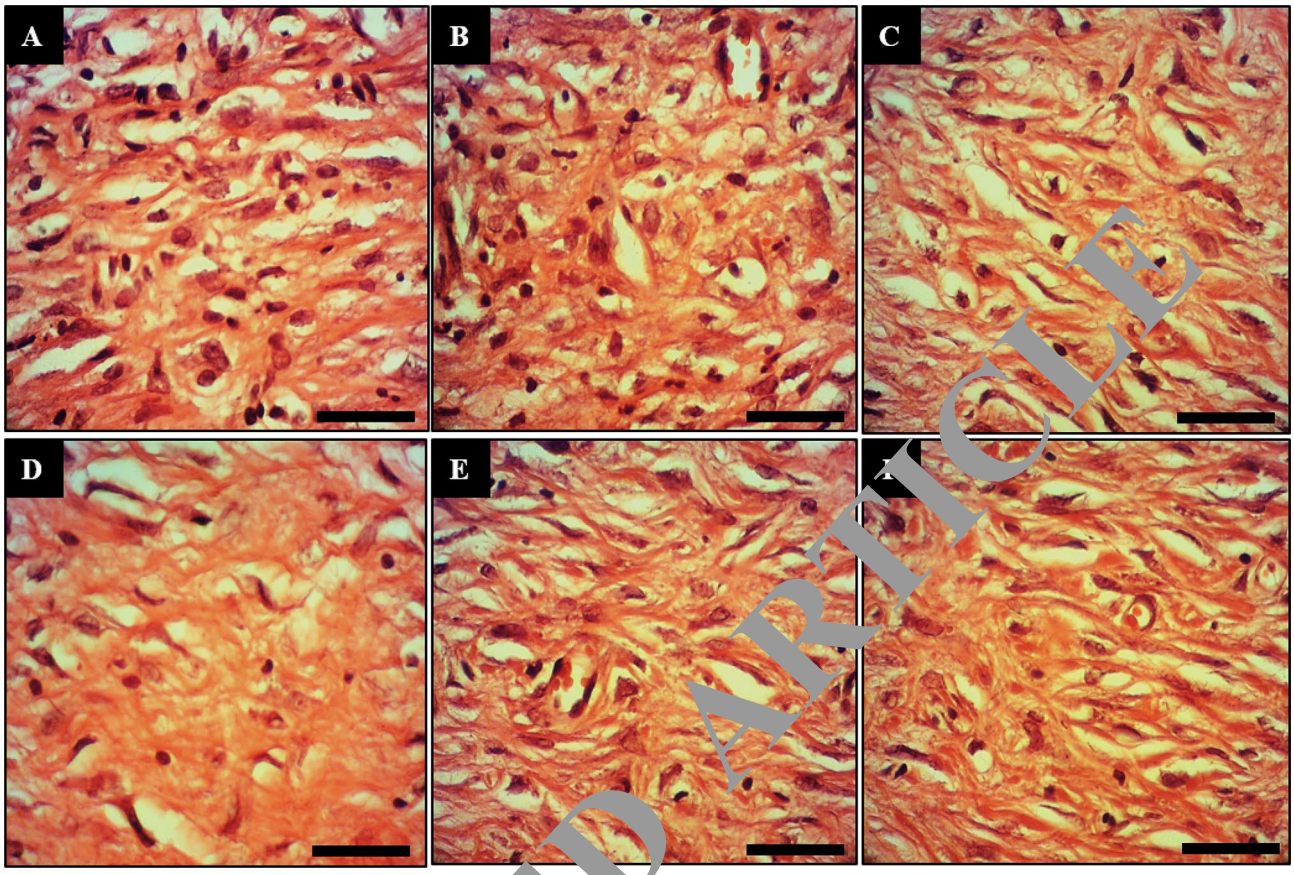

Figure 11. Longitudinal section of wounds of the control (**A**), basal ointment (**B**), tetracycline ointment (**C**), $Co(NO_3)_2$ ointment (**D**), *Z. clinopodioides* ointment (**E**), and CoNPs ointment (**F**) on 10 days post-injury. Scale bar: 600 µm. Magnification × 80.

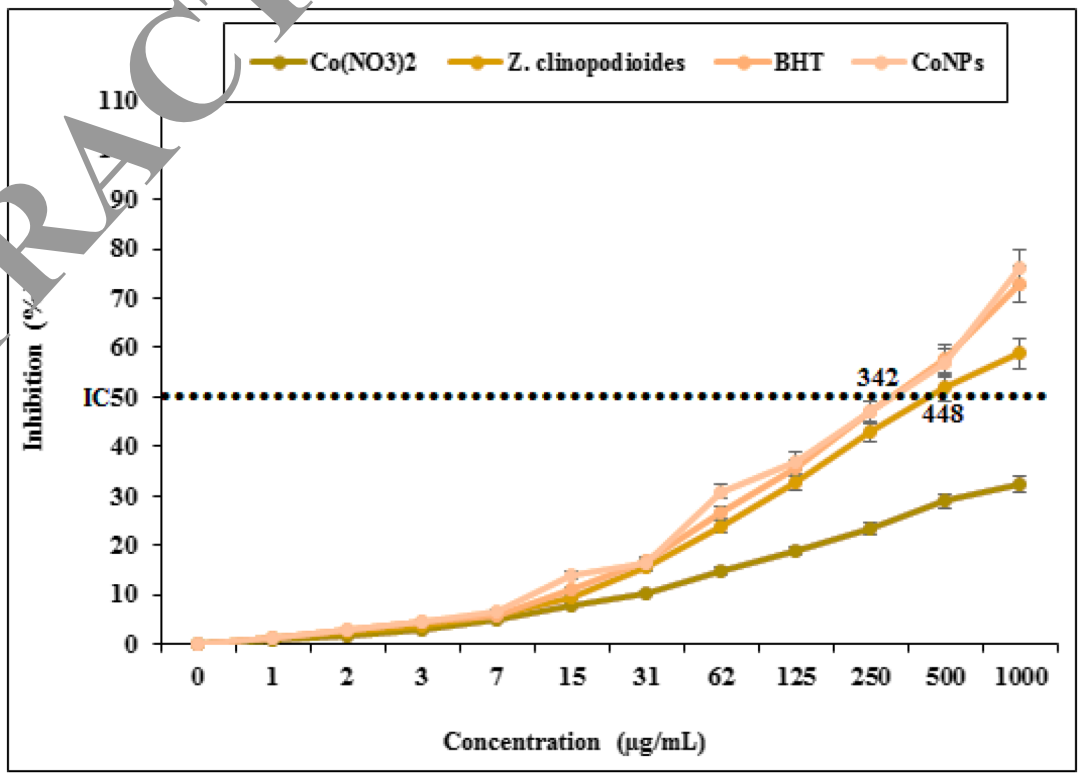

Figure 12. Antioxidant potential of $Co(NO_3)_2$, *Z. clinopodioides*, BHT, and CoNPs. *BHT* butylated hydroxyl toluene.

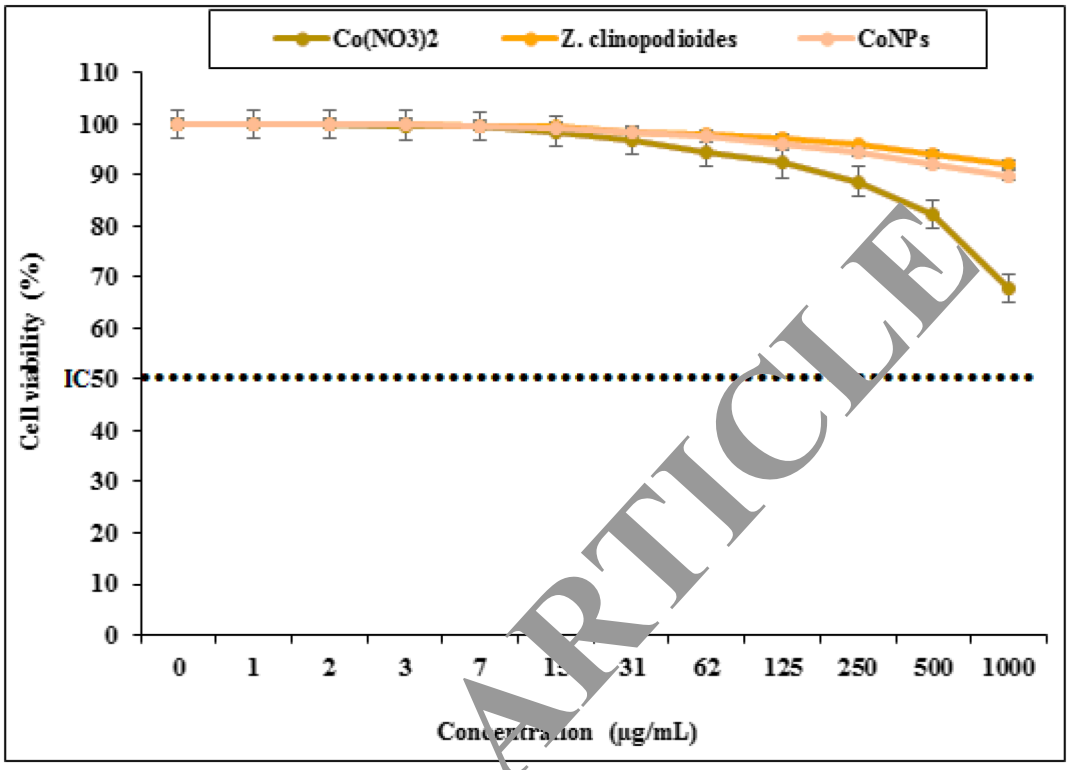

Figure 13. Percent viability measured on human umbilical vein endothelial cells after treatment with present $Co(NO_3)_2$, *Z. clinopodioides*, and CoNPs.

Enzymes	α-Gly (mM)	AChE (mM)	BChE (mM)
$Co(NO_3)_2$			
IC_{50}	15.86	[illegible]	1.32
r^2	0.976[illegible]	0.9[illegible]	0.9768
Ki + std	[illegible]51 + 2.73	0.42 ± 0.11	1.18 ± 0.17
CoNPs			
IC_{50}	11.[illegible]	1.24	2.20
r^2	[illegible]9371	0.9139	0.9861
Ki + std	15.[illegible]0 ± 3.10	1.04 ± 0.24	1.91 ± 0.38
[illegible]ndards (acarbose for α-Gly, tacrine for AChE and BChE)			
[illegible]	19.32	1.98	3.84
[illegible]^2	0.9646	0.9883	0.9812
[illegible] + std	23.21 ± 4.22	1.52 ± 0.41	3.12 ± 0.84

Table 10. Inhibition results of nanoparticles (CoNPs) on some metabolic enzymes (IC_{50} ve Ki values).

Received: 9 April 2020; Accepted: 3 July 2020
Published online: 22 July 2020

References

1. Ahmed, A., Mohamed, M., Moustafa, M. & Nazmy, H. Mass concentrations and size distributions measurements of atmospheric aerosol particles. *J. Nucl. Radiat. Phys.* **8**, 55–64 (2013).
2. Sintubin, L. *et al.* Lactic acid bacteria as reducing and capping agent for the fast and efficient production of silver nanoparticles. *Appl. Microbiol. Biotechnol.* **84**, 741–749 (2009).
3. Ball, V. Polydopamine nanomaterials: recent advances in synthesis methods and applications. *Front. Bioeng. Biotechnol.* **6**, 109. https://doi.org/10.3389/fbioe.2018.00109 (2018).
4. Hamelian, M., Zangeneh, M. M., Amisama, A., Varmira, K. & Veisi, H. Green synthesis of silver nanoparticles using *Thymus kotschyanus* extract and evaluation of their antioxidant, antibacterial and cytotoxic effects. *Appl. Organomet. Chem.* **32**, e4458. https://doi.org/10.1002/aoc.4458 (2018).
5. Hemmati, S. *et al.* Green synthesis and characterization of silver nanoparticles using Fritillaria flower extract and their antibacterial activity against some human pathogens. *Polyhedron* **158**, 8–14. https://doi.org/10.1016/j.poly.2018.10.049 (2019).

6. Sharma, V. K., Yngard, R. A. & Lin, Y. Silver nanoparticles: green synthesis and their antimicrobial activities. *Adv. Colloid Interface Sci.* **145**, 83–96. https://doi.org/10.1016/j.cis.2008.09.002 (2009).
7. Nadagouda, M. N. & Varma, R. S. Green and controlled synthesis of gold and platinum nanomaterials using vitamin B2: density-assisted self-assembly of nanospheres, wires and rods. *Green Chem.* **8**, 516–518. https://doi.org/10.1039/b601271j (2006).
8. Rajesh Kumar, B. & Saravanan, S. Effect of iso-butanol addition to diesel fuel on performance and emissions of a DI diesel engine with exhaust gas recirculation. Proc. Inst. *Mech. Eng. Part A J. Power Energy* **230**, 112–125. https://doi.org/10.1177/0957650915617107 (2016).
9. Raut, R. W., Kolekar, N. S., Lakkakula, J. R., Mendhulkar, V. D. & Kashid, S. B. Extracellular synthesis of silver nanoparticles using dried leaves of *Pongamia pinnata* (L) pierre. *Nano-Micro Lett.* **2**, 106–113. https://doi.org/10.1007/bf03353627 (2010).
10. Varma, R. S. Greener approach to nanomaterials and their sustainable applications. *Curr. Opin. Chem. Eng.* 1, 123 (2012).
11. Oliveira Mussel, R. L., Sá Silva, E., Costa, A. M. A. & Mandarim-De-Lacerda, C. A. Mast cells in tissue response to dentistry materials: an adhesive resin, a calcium hydroxide and a glass ionomer cement. *J. Cell. Mol. Med.* 17–178 https://doi.org/10.1111/j.1582-4934.2003.tb00216.x (2003).
12. Kumar, B., Vijayakumar, M., Govindarajan, R. & Pushpangadan, P. Ethnopharmacological approaches to wound healing—exploring medicinal plants of India. *J. Ethnopharmacol.* **114**, 103–113. https://doi.org/10.1016/j.jep.2007.08.010 (2007).
13. Guo, S. & DiPietro, L. A. Critical review in oral biology and medicine: factors affecting wound healing. *J. Dent. Res.* https://doi.org/10.1177/0022034509359125 (2010).
14. Souba, W. W. & Wilmore, D. *Diet and Nutrition in Case of the Patient with Surgery* 5th edn, 1589–1618 (Williams and Wilkins Press, Baltimore, 1999).
15. Rezvanipour, M., Pourzadehhosseini, F., Malekpour, R., Zarabi, A. & Kerman, J. The effect of mummy on some indices of wound healing in mice. *Univ. Med. Sci.* **14**, 77–267 (2007).
16. Goorani, S. *et al.* The aqueous extract of *Allium saralicum* R.M. Fritsch effective... heat induced anemia: experimental study on Wistar rats. *Orient. Pharm. Exp. Med.* **19**, 403–413. https://doi.org/10.1007/s13596-019-00361-5 (2019).
17. Zangeneh, M. M., Zangeneh, A., Tahvilian, R. & Moradi, R. Antidiabetic, hematoprotective and nephroprotective effects of the aqueous extract of *Falcaria vulgaris* in diabetic male mice. *Arch. Biol. Sci.* 655–664. https://doi.org/10.2298/ABS180222027Z (2018).
18. Hagh-Nazari, L. *et al.* Stereological study of kidney in streptozotocin-induced diabetic mice treated with ethanolic extract of *Stevia rebaudiana* (bitter fraction). *Comp. Clin. Pathol.* **26**, 455–46... https://doi.org/10.1007/s00580-016-2398-7 (2017).
19. Goorani, S. *et al.* Assessment of antioxidant and cutaneous wound healing effects of *Falcaria vulgaris* aqueous extract in Wistar male rats. *Comp. Clin. Pathol.* **28**, 435–445. https://doi.org/10.1007/s00580-018-2866-3 (2019).
20. Moradi, R. *et al.* Effect of aqueous extract of *Allium saralicum* R.M. Fritsch on fatty liver induced by high-fat diet in Wistar rats. *Comp. Clin. Pathol.* **28**, 1205–1211. https://doi.org/10.1007/s00580-018-2834-y (2019).
21. Jalalvand, A. R. *et al.* Chemical characterization and antioxidant, cytotoxic, antibacterial, and antifungal properties of ethanolic extract of *Allium saralicum* R.M. Fritsch leaves rich in linolenic acid, methyl ester. *J. Photochem. Photobiol. B Biol.* **192**, 103–112. https://doi.org/10.1016/j.jphotobiol.2019.01.017 (2019).
22. Sherkatolabbasieh, H. *et al.* Ameliorative effects of the ethanolic extract of *Allium saralicum* R.M. Fritsch on CCl 4-induced nephrotoxicity in mice: a stereological examination. *Arch. Biol. Sci.* **69**, 535–543. https://doi.org/10.2298/ABS160914129S (2017).
23. Zangeneh, M. M., Goodarzi, N., Zangeneh, A., Tahvilian, R. & Najafi, F. Amelioration of renal structural changes in STZ-induced diabetic mice with ethanolic extract of *Allium saralicum* R.M. Fritsch. *Comp. Clin. Pathol.* **27**, 861–867. https://doi.org/10.1007/s00580-018-2674-9 (2018).
24. Zhaleh, M. *et al.* Chemical composition and antibacterial effects of essential oil of *Rhus coriaria* fruits in the West of Iran (Kermanshah). *J. Essent. Oil-Bearing Plants* 21, 493–501. https://doi.org/10.1080/0972060X.2018.1462739 (2018).
25. Naghibi, F., Mosaddegh, M., Mohammadi Motamed, M. & Ghorbani, A. Labiatae family in folk medicine in Iran: from ethnobotany to pharmacology. *Iran. J. Pharm. Res.* **4**, 63–79. https://doi.org/10.22037/ijpr.2010.619 (2005).
26. Behravan, J. *et al.* Composition, antimycotic and antibacterial activity of *Ziziphora clinopodioides* Lam. essential oil from Iran. *J. Essent. Oil-Bearing Plants.* 339–345. https://doi.org/10.1080/0972060X.2007.10643565 (2007).
27. Sonboli, A., Mirjalili, M. H., Hadian, J., Ebrahimi, S. N. & Yousefzadi, M. Antibacterial activity and composition of the essential oil of *Ziziphora clinopodioides* subsp. *bungeana* (Juz.) Rech. F. from Iran. *Z. Naturforsch. Sect. C J. Biosci.* **61**, 677–680. https://doi.org/10.1515/znc-2006-9-1011 (2006).
28. Salehi, P., Sonboli, A., Eftekhar, F., Nejad-Ebrahimi, S. & Yousefzadi, M. Essential oil composition, antibacterial and antioxidant activity of the oil and various extracts of *Ziziphora clinopodioides* subsp. *rigida* (BOISS.) RECH. F. from Iran. *Biol. Pharm. Bull.* **28**, 1892–1897. https://doi.org/10.1248/bpb.28.1892 (2005).
29. Ghaisari, H. *et al.* Protection by *Ziziphora clinopoides* of acetic acid-induced toxic bowel inflammation through reduction of cellular lipid peroxidation and myeloperoxidase activity. *Hum. Exp. Toxicol.* **25**, 325–332. https://doi.org/10.1191/0960327105ht626oa (2006).
30. Kürkcüoğlu, G. E., Konyalioglu, S. & Ozturk, B. Essential oil composition and antioxidant activity of endemic *Ziziphora taurica* subsp. *cleonioides*. *Fitoterapia* **73**, 716–718. https://doi.org/10.1016/S0367-326X(02)00244-7 (2002).
31. Oganesyan, G. B., Galstyan, A. M., Mnatsakanyan, V. A., Paronikyan, R. V. & Ter-Zakharyan, Y. Z. Phenolic and flavonoid compounds of *Ziziphora clinopodioides*. *Chem. Nat. Compd.* **27**, 247. https://doi.org/10.1007/BF00629776 (1991).
32. Belyaev, N. F. & Demeubaeva, A. M. Chromatographic study of the composition of the essential oil of *Ziziphora clinopodioides*, a vicarious form of *Origanum* vulgare. *Chem. Nat. Compd.* **35**, 52–54. https://doi.org/10.1007/BF02238209 (1999).
33. Zangeneh, M. M., Norouzi, H., Mahmoudi, M., Goicoechea, H. C. & Jalalvand, A. R. Fabrication of a novel impedimetric biosensor for label free detection of DNA damage induced by doxorubicin. *Int. J. Biol. Macromol.* **124**, 963–971. https://doi.org/10.1016/j.ijbiomac.2018.11.278 (2019).
34. Ghashghaii, A., Hashemnia, M., Nikousefat, Z., Zangeneh, M. M. & Zangeneh, A. Wound healing potential of methanolic extract of *Scrophularia striata* in rats. *Pharm. Sci.* **24**, 256–263. https://doi.org/10.15171/PS.2017.38 (2017).
35. MahdiZangeneh, M., Zangeneh, A., Salmani, S., Jamshidpour, R. & Kosari, F. Protection of phenylhydrazine-induced hematotoxicity by aqueous extract of *Ocimum basilicum* in Wistar male rats. *Comp. Clin. Pathol.* https://doi.org/10.1007/s00580-018-2845-8 (2018).
36. Koyyati, R., Rao Kudle, K. & Rudra Manthur Padigya, P. Evaluation of antibacterial and cytotoxic activity of green synthesized cobalt nanoparticles using *Raphanus sativus* var. *longipinnatus* leaf extract. *Int. J. PharmTech. Res.* **9**, 466–472 (2016).
37. Ahmed, K., Tariq, I., Siddiqui, S. U. & Mudassir, M. Green synthesis of cobalt nanoparticles by using methanol extract of plant leaf as reducing agent. *Pure Appl. Biol.* **5**, 453–457. https://doi.org/10.19045/bspab.2016.50058 (2016).
38. Arulmozhi, V., Pandian, K. & Mirunalini, S. Ellagic acid encapsulated chitosan nanoparticles for drug delivery system in human oral cancer cell line (KB). *Colloids Surf. B Biointerfaces* **110**, 313–320. https://doi.org/10.1016/j.colsurfb.2013.03.039 (2013).
39. Hosseinimehr, S. J. *et al.* The radioprotective effect of *Zataria multiflora* against genotoxicity induced by γ irradiation in human blood lymphocytes. *Cancer Biother. Radiopharm.* **26**, 325–329. https://doi.org/10.1089/cbr.2010.0896 (2011).
40. Clinical and laboratory standards institute (CLSI). M7-A7. 26(2) (2006).
41. Kim, D. H., Nikles, D. E., Johnson, D. T. & Brazel, C. S. Heat generation of aqueously dispersed $CoFe_2O_4$ nanoparticles as heating agents for magnetically activated drug delivery and hyperthermia. *J. Mag. Mag. Mater.* **320**, 2390–2396 (2008).

42. Sanpo, N., Berndt, C. C., Wen, C. & Wang, J. Transition metal-substituted cobalt ferrite nanoparticles for biomedical applications. *Acta Biomater.* **9**, 5830–5837 (2013).
43. Zheng, L., He, K., Xu, C. Y. & Shao, W. Z. Synthesis and characterization of single-crystalline $MnFe_2O_4$ nanorods via a surfactant-free hydrothermal route. *J. Mag. Mag. Mater.* **320**, 2672–2675 (2008).
44. Tian, S., Shi, Y., Yu, Q. & Upur, H. Determination of oleanolic acid and ursolic acid contents in *Ziziphora clinopodioides* Lam. by HPLC method. *Pharmacogn. Mag.* **6**, 116–119. https://doi.org/10.4103/0973-1296.62898 (2010).
45. Baghayeri, M., Mahdavi, B., Hosseinpor-Mohsen Abadi, Z. & Farhadi, S. Green synthesis of silver nanoparticles using water extract of *Salvia leriifolia*: antibacterial studies and applications as catalysts in the electrochemical detection of nitrite. *Appl. Organomet. Chem.* **32**, e4057. https://doi.org/10.1002/aoc.4057 (2018).
46. Isaac, R. S. R., Sakthivel, G. & Murthy, C. Green synthesis of gold and silver nanoparticles using averrhoa bilimbi fruit extract. *J. Nanotechnol.* https://doi.org/10.1155/2013/906592 (2013).
47. Gingasu, D. *et al.* Synthesis of nanocrystalline cobalt ferrite through soft chemistry methods: a green chemistry approach using sesame seed extract. *Mater. Chem. Phys.* **182**, 219–230. https://doi.org/10.1016/j.matchemphys.2016.07.0[illegible]2016)
48. Matinise, N., Mayedwa, N., Fuku, X. G., Mongwaketsi, N. & Maaza, M. Green synthesis of cobalt (II, III) oxide nanoparticles using *Moringa oleifera* natural extract as high electrochemical electrode for supercapacitors application. *AIP Conf. Proc.* https://doi.org/10.1063/1.5035543 (2018).
49. Lazarus, G. S. *et al.* Definitions and guidelines for assessment of wounds and evaluation of healing. *Wound Repair Regen.* **2**, 165–170. https://doi.org/10.1046/j.1524-475X.1994.20305.x (1994).
50. Phillips, G. D., Whitehead, R. A. & Knighton, D. R. Initiation and pattern of angiogenesis in wound healing in the rat. *Am. J. Anat.* **192**, 257–262. https://doi.org/10.1002/aja.1001920305 (1991).
51. Caetano, G. F., Fronza, M., Leite, M. N., Gomes, A. & Frade, M. A. C. Comparison of collagen content in skin wounds evaluated by biochemical assay and by computer-aided histomorphometric analysis. *Pharm. Biol.* **54**, 2555–2559. https://doi.org/10.3109/13880209.2016.1170861 (2016).
52. Azhdari-Zarmehri, H. *et al.* Assessment of effect of hydro-alcoholic extract of scrophularia striata on burn healing in rat. *J. Babol Univ. Med. Sci.* **16**, 42–48. https://doi.org/10.18869/ACADPUB.JBUMS.16[illegible] (2014).
53. Dwivedi, D., Dwivedi, M., Malviya, S. & Singh, V. Evaluation of wound healing, antimicrobial and antioxidant potential of Pongamia pinnata in wistar rats. *J. Tradit. Complement Med.* **7**, 79–85 (2017).
54. Shivananda Nayak, B., Isitor, G., Davis, E. M. & Pillai, G. K. T[illegible]evid[illegible]based wound healing activity of *Lawsonia inermis* Linn.. *Phyther. Res.* **21**, 827–831. https://doi.org/10.1002/ptr.2181 (20[illegible]
55. Oryan, A., Tabatabaei Naeini, A., Moshiri, A., Mohammadalipour, [illegible]-Tabandeh, M. R. Modulation of cutaneous wound healing by silymarin in rats. *J. Wound Care.* **21**, 457–464. http[illegible]doi.org/10.[illegible]2968/jowc.2012.21.9.457 (2012).
56. Dong, Y. L., Fleming, R. Y., Yan, T. Z., Herndon, D. N. & Wa[illegible]P. Effect of ibuprofen on the inflammatory response to surgical wounds. *J. Trauma* **35**, 340–343. https://doi.org/10.1097/00005373-199309000-00002 (1993).
57. Koh, T. J. & DiPietro, L. A. Inflammation and wound healing: the role of the macrophage. *Expert Rev. Mol. Med.* https://doi.org/10.1017/S1462399411001943 (2011).
58. Foschi, D. *et al.* The effects of oxygen free radicals on wound healing. *Int. J. Tissue React.* **10**, 373–379 (1988).
59. Robards, K., Prenzler, P. D., Tucker, G., Swatsitang, P. & Glover, W. Phenolic compounds and their role in oxidative processes in fruits. *Food Chem.* **66**, 401–436. https[illegible].org/[illegible].1016/S0308-8146(99)00093-X (1999).
60. Geethalakshmi, R., Sakravarthi, C., Kritika, T., Arul Kirubakaran, M. & Sarada, D. V. L. Evaluation of antioxidant and wound healing potentials of *Sphaeranthus amaranthoides* Burm.f. *Biomed Res. Int.* https://doi.org/10.1155/2013/607109 (2013).
61. Zengin, M. *et al.* Novel thymol bearing oxypropanolamine derivatives as potent some metabolic enzyme inhibitors—their antidiabetic, anticholinergic and antibacterial potentials. *Bioorg. Chem.* **81**, 119–126. https://doi.org/10.1016/j.bioorg.2018.08.003 (2018).
62. Taslimi, P. *et al.* Diarylmethanon[illegible]methanon[illegible]ophenol and diarylmethane compounds: discovery of potent aldose reductase, α-amylase and α-glycosidase inhibitors as new therapeutic approach in diabetes and functional hyperglycemia. *Int. J. Biol. Macromol.* **119**, 857–863. https://doi.org/[illegible]1016/j.ijbiomac.2018.08.004 (2018).

Acknowledgements

ThisAckn[illegible]k was supported by the grants from the National Natural Science Foundation of China (No. 81200836) a[illegible]the National Undergraduate Innovation and Entrepreneurship Training Program (No. S201[illegible]2026).

Author contributions

[illegible]M.Z., B.M., and F.S. organized all experiments and wrote the manuscript.; H.H., S.P., A.Z., P.T., and N.S., P.T. a[illegible], performed all experiments. They have also drawn the figures.

Competing interests

The authors declare no competing interests.

Additional information

Correspondence and requests for materials should be addressed to B.M., M.M.Z. or F.S.

Reprints and permissions information is available at www.nature.com/reprints.

Publisher's note Springer Nature remains neutral with regard to jurisdictional claims in published maps and institutional affiliations.